

FINAL PROGRESS REPORT

Economical and Stable Operability of Industrial Multi- Stage Flash Processes

(Project number 26/422)

Prepared by: Dr. Emad Ali
Chemical Engineering Department
King Saud University

Acknowledgment

The investigator is very grateful to SABIC for supporting this project financially under the program for funding short-term academic research projects. The investigator would also like to thank the general directorate of research center at the college of engineering for their support, continuous follow up and patience throughout the project duration. I would like to emphasize the benefit and advantage of this program, which enables the scientist and scholars to manifest their research ideas into realistic application.

The investigator would like also to thank the chemical engineering department for providing lab facilities such as space and utilities in addition to laboratory materials and accessories.

Summary

This work deals with expanding the knowledge about the operation of multi-stage flash (MSF) desalination processes. This is achieved through stability and steady state analysis conducted on a simulated model for the MSF plant. The model is developed and validated using steady state plant data. The stability analysis is based on the eigenvalues of the linearized version of the model, which revealed that the MSF plant is normally internally stable. The steady state analysis investigated the effect of each process input on the process key variables. Combinatorial effect of two inputs at a time is also examined. The steady state analysis is found useful to locate economically favorable operating conditions and to locate conditions at which undesirable brine level may occur. The steady state analysis is also useful to study the controllability of the MSF plant, which helps in enhanced control design.

The investigation includes studying the set point optimization of the MSF plant. This is achieved by optimizing the steady state model of the plant to determine the optimal operating conditions. The objective function is designed such that it determines the feasible values for the plant operational parameters that maximize the performance ratio. The investigation also includes studying the dynamic behavior of the process during open-loop and closed-loop operations. The dynamic analysis in both cases focuses on investigating the source and existence of operation stability due to blow-through or liquid pileup. The entire analysis is based on simulation of a previously validated model for the MSF plant.

الملخص

يهدف هذا البحث على إثراء المعرفة بمشاكل تشغيل محطات تحلية مياه البحر التي تستخدم طريقة التبخير الومضي المتعدد المراحل. و يعتمد البحث على دراسة الإستقرارية للنظام في حالة الثبات باستخدام نموذج رياضي لمخطة التحلية الذي تم تطويره سابقا و التأكد من مطابقتة للواقع عن طريق مقارنته ببيانات معملية في حالة الثبات. و قد أوضحت تحاليل الإستقرارية المبنيه على جذور النموذج الرياضي بأن محطات التحلية تعتبر عمليات مستقرة بخلاف ماهو معروف عنها. كما تم دراسة تأثير عدد من مدخلات عملية التحلية على عدد من المستخرجات في حالة الثبات مع الزمن (التحليل الإستاسي). و قد ساعدت هذه التحليلات على تحديد مناطق تشغيل إقتصادية و تحديد

ظروف تشغيل غير مرغوب فيها فيما يخص إرتفاع السوائل داخل حجرات التبخير الومضي. كما أن التحليل الإستاسي يساعد على فهم خاصية التحكمية لعملية التحلية مما يساعد على تطوير نظام التحكم بشكل أفضل.

كما شمل البحث دراسة أمثلية ظروف التشغيل و بالتالي يمكن تحديد ظروف التشغيل المثلى لعملية التحلية من حيث زيادة معدل الكفاءة (نسبة الإنتاج الى إستهلاك الطاقة) مع المحافظة على إستقرارية و ثبات عملية التحلية. و تعتمد دراسة الأمثلية على حل مسألة الأمثلية الرياضية بناءا على النموذج الرياضي لعملية التحلية تحت ظروف التشغيل الثابتة مع الزمن. كما شمل البحث دراسة حالة التغير مع الزمن (التحليل الدينامي) لعملية التحلية في حالي الدائرة المفتوحة و الدائرة المغلقة (أي في وجود نظام التحكم). و قد تم التركيز خلال التحليلات الدينامية على تشخيص وجود و مصادر ظروف اللاستقرارية في إرتفاع السوائل داخل حجرات التبخير.

Introduction

It is well known that fresh water is not available in every part around the world. Moreover, some of the available water resources require special form of treatment. This situation created water shortages in many nations around the world. As a result, MSF desalination became the main source of fresh water for domestic, industrial and agricultural consumption. Some statistics on the world capacity of desalinated water and the growing number of MSF desalination units can be found elsewhere [1].

The major advantage of MSF is that evaporation occurs due to pressure vacuum in the bulk fluid away from the surface of hot tubes. Therefore, loss of efficiency and material due to scale and corrosion is avoided. The paramount importance of desalination in producing potable water, draw the attention of many engineers and researchers to enhance the operation of such plants in the most efficient manner possible. For this reason, several research efforts were devoted for the modeling and simulation of MSF plants. Steady state and dynamic modeling were reported [2]. Similarly many researchers studied the empirical modeling of MSF plants using real time process data [3-6].

MSF plant is notorious of being prone to instability [7]. Disturbances in steam supply, seawater temperature or process load can lead to instability of the brine level in the evaporator. Instability can cause undesirable carry over of brine into distillate or blow-through of brine in stages. This situation can lead to loss of efficiency or frequent shutdown. In addition, there is a high potential to improve the MSF operation in order to enhance its performance ratio. Several attempts were reported to properly understand the MSF operation. Hussain et. al [8] used their validated process model to study the effect of operation parameter on the brine level dynamics. They also carried steady state analysis to develop operating envelope and locate the conditions for carryover or blow-through. Similarly, Thomas et. al. [2] also simulated the brine level dynamics to changes in steam flow in an attempt to understand its behavior. They concluded that large step changes in steam flow should be avoided because they may lead carryover or blow-through situations. Bodendieck et. al. [9] studied the effect of orifice design and configuration on the stability of brine level. They also defined the permissible operation range for each orifice type. Analysis was also

conducted to demonstrate the effect of operation parameters on the brine level at steady state. In practice, the level instability is handled by controlling the level of the last stage [7]. Nevertheless, the brine level instability is not yet properly tackled through systematic and theoretical analysis. The origin of this instability is not yet well understood. Moreover, besides generating safe operation, potential for optimal operation of the MSF plants also exists. The MSF plant consists of many stages with several numbers of states with overlapping effects, which makes understanding its behavior more complex. Therefore it is essential to understand the steady state and the transient behavior of the process in the open-loop and closed-loop modes. This work focuses on this issue. The steady state model of the process will be used to investigate the internal stability of the process. A comprehensive steady state analysis will be conducted. This will involve determining the influence of admissible range of each plant operation parameters on the process major outputs at steady state. The analysis will be carried out in open-loop and closed-loop modes. The combined effect of two operation parameters on the process steady state will be also examined. The obtained information can be useful to define which operation parameter has the most positive effect on the plant economic, and which has the most adverse effect on the brine level.

The steady state analysis is helpful in bracketing the good operating regions of maximum production or performance ratio and in isolating bad operating conditions of undesirable brine level such as blow-through or carryover. However, the favorable operating conditions were determined for each operation parameter separately. It is of interest to locate the optimum value for the entire operation parameters that maximize certain performance index. In addition, it is important to consider the physical bounds imposed on the plant parameters and to satisfy certain constraints such as those induced by requiring safe brine level conditions. In this case, the optimum operating condition is cast as a multivariable constrained optimization problem and solved by available numerical techniques. Optimization of an MSF plant is investigated by Kraus and Hassan [10]. They outlined the general objective and formulation of the optimization problem and discussed their experience on the online implementation of the optimization module on the Distributed Control System. No graphical results are shown in their work.

On the other hand, the MSF process passes through transient response due to severe disturbance or excessive set point changes. The MSF dynamic is complex due to nonlinearity and to the large number of stages. The effect of a perturbation that occurs upstream on the process dynamic is transmitted progressively from one stage to another. Each flash evaporator introduces a capacitance to the process dynamic, which presents a time lag. The time lag accumulates progressively with the train of stages creating a larger time delay at the down stream stages. The information gained from the steady state analysis determines only the process state values at steady state for a given perturbation in the operation parameter. Even if the values for the process states are found acceptable or favorable at steady state, they do not reveal what happens during the transient period. Because of time delay, the process states especially the brine levels may exhibit serious overshoot or inverse response. Therefore, it is important to examine the dynamic behavior of the process states during step changes in the process operation parameters. The dynamic analysis will be conducted in open-loop and closed-loop modes of operation. Few efforts dealing with dynamic simulation of MSF plants have been reported. Zhang and Wang [11] studied the effect of step changes in the recycle brine flow and steam flow on the dynamic response of the brine level. The analysis is conducted while the plant is operating in an open-loop mode. Similarly, Thomas et. al. [12] examined the effect of positive and negative disturbances in the steam flow. The open-loop response of the brine level to these specific disturbances is discussed. Hussain et. al. [13] investigated the transient response of the brine level to an upset in the steam flow. They examined and compared two cases. In one case the brine level of the last stage is allowed to vary freely and in the other case it is controlled. They also examined the effect of a small perturbation in steam temperature on the brine level response. In that test, the brine level of the last stage is controlled. In the above research works the effect of only a single variable or at most two process inputs is examined. Furthermore, in most of the cases, the analysis is carried out in open-loop mode. Even when closed-loop operation is considered, only a single variable is controlled. In contrast, the analysis covered in this work is more comprehensive.

The information provided by the optimization and dynamic analysis serves as useful tool for engineers and operators. For example, an engineer can utilize the

results in this work to select most profitable conditions and avoid hazardous operation. Such systematic analysis enables the engineer to make sound decisions.

Process Description

In a typical MSF plant shown in Fig. 1 we can distinguish between three basic sections: heat rejection section, heat recovery section and the brine heater. On leaving the first (warmest) rejection stage the feed stream is split into two parts, reject sea water which passes back to the sea and a make up stream, which is then recycled back to the flash section of the last stage. A recycle stream, which is drawn from the last stage, passes through a series of heat exchangers, its temperature rises as it proceeds towards the heat input section of the plant. Passing through the brine heater the brine temperature is raised from the feed temperature at the inlet of the brine heater to a maximum value approximately equals to the saturation temperature at the system pressure. The brine then enters the first heat recovery stage through an orifice thus reducing the pressure. As the brine was already at its saturation temperature it will become superheated for a lower pressure and flashes to give off water vapor. The vapor then passes through a wire mesh (demister) to remove any entrainment brine droplets and onto a heat exchanger where the vapor is condensed and drips into a distillate tray. The process is then repeated all the way through the plant as both brine and distillate enter the next stage which is at a lower pressure. The concentrated brine is divided into two parts as it leaves the plant, a blow-down, which is pumped back to the sea and the recycle stream.

Process Model

The design and analysis of process operation requires the use of a rigorous model of the MSF plant. A first principle model for a 22 stages MSF plant was developed and validated [10]. The specific plant consists of 3 rejection section stages and 19 recover section stages. In the following a summary of the developed model is given. Each plant stage is shown in Fig. 2. The process is therefore defined by nine variables: brine pool height (L_j), brine flow rate (B_j), salt mass fraction (X_j), brine temperature (T_{Bj}), distillate flow rate (D_j), distillate temperature (T_{Dj}), coolant temperature (T_{Cj}), vaporization rate (V_j) and stage pressure (P_j). Furthermore and in order to minimize the size of the model the liquid levels, except that for the last stage, and the temperature dynamics in the distillate tray are not included in the modeling.

The dynamics for the salt concentration is also excluded because they have no direct effect on the other process states except through physical properties of the brine such as density and heat capacity. Our simulations revealed that the physical properties vary between +1 and -1 % over the plant temperature range due to changes in salt concentration. The mass holdup of the cooling brine inside the condenser tubes is assumed constant. The following mass and energy equations are written for each stage [14]:

Stage j (except the last stage)

- Mass balance of brine pool

$$\rho_{B,j} A_B \frac{dL_j}{dt} = B_{j-1} - B_j - V_j \quad (1)$$

- Energy balance of brine pool

$$\rho_{B,j} A_B L_j C_{p_{B,j}} \frac{dT_{Bj}}{dt} = B_{j-1} C_{p_{B,j}} (T_{B,j-1} - T_{B,j}) - V_j (\lambda_{c,j} - C_{p_{B,j}} (T_{B,j} - T_o)) \quad (2)$$

- Mass balance in distillate tray

$$D_j = D_{j-1} + V_j \quad (3)$$

- Energy balance of condenser tubes

$$M_{C,j} C_{p_{C,j}} \frac{dT_{C,j}}{dt} = B_0 C_{p_{C,j}} (T_{C,j+1} - T_{C,j}) + U_j A_{HC} \Delta T_j \quad (4)$$

$$U_j A_{HC} \Delta T_j = V_j \lambda_j \quad (5)$$

(for the rejection section the see water feed W_F is used instead of B_0 in the last equation)

Last stage, N

- Mass balance in brine pool

$$\rho_{B,j} A_B \frac{dL_N}{dt} = B_{N-1} - B_N - V_N + W_{mk} - B_0 \quad (6)$$

- Energy balance in brine pool

$$\rho_{B,j} A_B L_N C_{p_{B,j}} \frac{dT_{B,N}}{dt} = B_{N-1} C_{p_{B,j}} (T_{B,N-1} - T_{B,N}) - V_N (\lambda_N - C_{p_{B,j}} (T_{B,N} - T_o)) + W_{mk} C_{p_{B,j}} (T_{C,3} - T_{B,N})$$

(7)

- Mass balance in distillate tray

$$D_N = D_{N-1} + V_N \quad (8)$$

- Energy balance of condenser tubes

$$M_{C,N} C_{pC,N} \frac{dT_{C,N}}{dt} = W_F C_{pC,N} (T_F - T_{C,N}) + U_N A_{HR} \Delta T_N \quad (9)$$

$$U_N A_{HR} \Delta T_N = V_N \lambda_N \quad (10)$$

Splitter

$$W_F = \text{Rej} + W_{mk} \quad (11)$$

Brine Heater

- Energy Balance equation

$$M_{BH} C_{pB,j} \frac{dT_{B0}}{dt} = B_0 (C_{pC,1} T_{C,1} - C_{pB0} T_{B0}) + W_s \lambda_s \quad (12)$$

In the above model equations the brine flow and the brine level in each stage are correlated as follows:

$$B_j = w L_j K_j \sqrt{\rho_{B,j} (P_{j-1} - P_j + \rho_{B,j} g (L_j - Ch_j))} \quad (13)$$

similarly, the distillate flow is correlated to the distillate level as follows:

$$D_j = C_{D,j} \sqrt{\rho_{D,j} g L_{D,j}} \quad (14)$$

The temperature difference used in the above energy balances is defined as follows:

$$\Delta T_i = T_{B,i} - 0.5(T_{C,i} + T_{C,i+1})$$

Note that λ_j is computed at T_{Bj} while $\lambda_{c,j}$ is computed at the distillate temperature, which is assumed to be equal T_{Bj} minus the boiling point rise at the j^{th} stage (BPR_j). In the original model [14], the physical properties for each stage in the above model, i.e.

$\rho, C_p, \lambda, U, M_c, M_{BH}, BPR$ and the vapor pressure (P) are estimated through empirical correlation.. Industrial values were used for the plant design parameters such as $C, h, A_B, A_{HC}, A_{HR}$ and w . Moreover, realistic values for the size and number of tubes were used in computing U, M_c and M_{BH} . The definition of all parameters of the model equations is given in the nomenclature. The nominal operating condition for the plant upon which the model is validated is given in Table 1. The model output is validated against available plant steady state data such as Brine temperature, Condenser temperature, inter-stage brine flow and inter-stage distillate flow rates. The latter flow rates were used also to verify the level-flow correlation, i.e. Eqns. (13) and (14). Although the overall heat transfer coefficient (U) can be computed from a given correlation, some degree of uncertainty still exists. Therefore, its value was adjusted so that exact matching of the plant data is obtained. In a typical MSF plant, the upstream distillate flashes back to the tube bundle when it enters the new stage at lower temperature. However, this amount is assumed very small and thus it is ignored in equation 3 above. Note that the symbols L and L_B denote the same variable and they will be used interchangeably hereafter.

Stability Analysis

Stability of the brine height and consequently of the overall process is very crucial issue. It is reported that plant disturbances may cause level instability in the form of carry over of brine into the distillate or blow through interstage orifice. However, the level instability is not tackled clearly. It is not confirmed whether the cause of instability is the internal characteristics of the process or the plant improper operation. Distinction between *internal* instability and *operational* instability should be clarified. The internal instability is an inherent characteristic of the dynamic model of the process at a specific operating condition. This characteristic is represented mathematically by the poles or the eigen-values (nodes) of the linearized mathematical system of the process. A positive node is an indication of an unstable process. The unstable process can not be kept operating at the unstable node without the use of control system and moreover any infinitesimal upset causes the process dynamic to drift away or runaway to another stable node if exists. The operational instability on the other hand does not necessarily indicate unstable process. It usually indicates undesirable operation. For example, the MFS plant may operate at stable low brine level. However, if the level is lower than the orifice opening, blow through

occurs, which is not a favorable practice. Similarly, high steady brine height may cause carry over reducing the efficiency. In addition, stable level fluctuation may require simultaneous adjustment of the orifice height, which is another unfavorable operation.

In this section, the internal stability of the brine level is examined. To examine the internal stability of the process, the model is first linearized in the neighborhood of a singular point (steady state point). The linearized model is simply the Jacobian of the state equations (Eqns. 1-12). The eigen-values for the Jacobian matrix can then be evaluated using any numerical technique. If the real part of any node is positive, the system is considered unstable.

In general, the dynamic of the brine level in the flashing chambers resembles the dynamic of the level of interacting storage tanks in series. It is well known that such process exhibits over-damped internally stable dynamic when the outlet flow is left to vary freely with height. Consequently, the brine level should also be internally stable if the blow-down is left flowing out freely. In fact, the brine can not flow out of the last stage spontaneously because the stage pressure is less than atmospheric. For this reason a pump is usually used to draw the brine down. In this case the process becomes unstable unless the blow-down flow is used as manipulated variable to control the last stage level. Moreover, the dynamic equations for the brine level (Eqns. 1,6) contain the vapor rate variable. If the latter is a function of the brine level, then the process dynamic can not be compared to that of storage tanks in series and the stability analysis may differ. Basically, when the vapor rate is ignored and the blow-down is free, the Jacobian matrix for the level state equations is a lower triangular matrix. The eigen-values are then the diagonal elements of the Jacobian, which are the derivatives of the brine flow with respect to the level. By simple glance at equation 13 it can be easily inferred that the diagonal elements are negative, i.e. the process is internally stable. However, it remains to examine the inclusion of the vapor rate on the eigen-values of the Jacobian matrix.

The given MSF model contains 67 state equations, which covers 22 brine level states, 22 brine temperature states, 22 condenser temperature states and the top brine temperature state. The three sets of state variables, i.e. L , T_B , and T_C , are correlated

through the vaporization rate, V . Therefore to investigate the effect of the vapor rate on the stability of the brine level, analytical solution of the vapor rate in terms of the other states should be derived and then substituted in the level state equations. However, obtaining analytical solution for the full model of 67 states is a difficult task. To simplify the mathematical treatment, the following stability analysis that includes the vapor rate is based on a 3-stages plant. In this case the recovery section has 2 stages and the rejection section a single stage. The reduced model is given in the appendix. Assuming steady state condition for T_B and T_C states and constant physical properties and by algebraic manipulation the level state equations for the 3-stages model can be shown to be:

$$\begin{aligned}\rho_B A_B \dot{L}_1 &= B_0 - B_1 - B_0 b_2 \frac{Cp_B}{\lambda_1} \\ \rho_B A_B \dot{L}_2 &= B_1 - B_2 - b_2 \frac{W_s \lambda_s}{\lambda_2 (B_1 b_1 + B_0 b_2)} \\ \rho_B A_B \dot{L}_3 &= B_2 - B_3 - B_0 + W_{mk} - W_F a_2 \frac{W_s \lambda_s B_1 B_2}{B_0 \lambda_3 m (B_1 b_1 + B_0 b_2)}\end{aligned}$$

where a_2 , b_2 and m are defined in the appendix. According to the above equations, it is clear that the vapor rate does not affect the stability analysis of the level states. In fact, the Jacobian is still a lower triangular matrix with its diagonal elements are the derivative of the brine flow of each stage with respect to its corresponding brine level. Therefore, utilizing the definition of the brine flow in equation (13), the process is considered internally stable. Note that in deriving the above equations, $Cp_B = Cp_F$ and $\lambda_s = \lambda$ are considered. This assumption does not affect the structure of the Jacobian or the type of the resulted eigen-values. Although the resulted analysis is based on reduced model it can be generalized to the full model because the process model is triangular and symmetric. To further confirm the internal stability of the full MSF model without any idealization, the Jacobian will be created and its eigenvalues will be evaluated at each singular point. The Jacobian and the eigenvalues are computed numerically. The stability analysis is then based on the computed eigenvalues. This procedure is considered in the next section.

Steady State Analysis

The MSF process model consists of several variables that represent its operating state. The major state variables are the brine temperature (T_B), the fluid temperature flowing inside the condenser (T_C), the brine flow rate or the brine level (B/L_B), the distillate flow rate or the distillate level (D/L_D) in each flashing stage and the brine temperature entering the first stage (T_{B0}). The brine flow states include the blow-down flow (B_D), which is the brine flow leaving the last stage. Similarly, the distillate flow states include the distillate product (W_D), which is the distillate flow rate leaving the last stage. Note that the flow states and the level states whether for the brine or the distillate are interrelated, therefore, they can not be treated as fully independent states. The MSF model contains other states variable which are also not fully independent such as the vapor pressure, the vapor rate and distillate temperature in each stage. In addition, the MSF process has several forcing function or external inputs. These inputs are the sea water feed rate (W_F) entering the condenser tube of the last stage, the temperature of the sea water feed (T_F), The brine reject flow (Rej), the recycle brine flow (B_0), the steam the flow to the brine heater (W_s), and the steam temperature (T_s). The makeup flow rate (W_{mk}) is a dependent input variable and equals the difference between W_F and Rej. Some other MSF configuration has an extra input variable, which is the re-circulating flow. This input is not considered here.

The set of values for the process inputs specifies exactly the process states. This means that any combination of the input values, a unique steady state value for the process states can be determined. These steady state values specify the process operating condition. Determining the plant operating condition is important for the safe and economical operation of the process. For example, an optimum operating condition that maximizes the distillate product, minimizes the steam consumption or maximizes the performance ratio can be determined offline. The performance ratio is the ratio of the distillate product to the steam consumption. Alternatively, controllability region for the process operation can also be determined. The controllability region can help in defining undesirable operating conditions that might bring the plant to operational instability or to the edge of process constraints. Therefore it is important to study the effect of the process inputs on a specific process key variable such as W_D , B_D , and L_B . The first process variable affects the process

economy directly. The other two process variables play important role in the stability of the plant. The brine level is known to undergo phases of unstable operational conditions such as blow through or flooding, which usually result from sudden changes in the process inputs.

Open-loop simulation:

It is interesting to investigate the effect of each process input on the plant states. Figures 3-7 simulate the results of this investigation. In each figure the model state equations are solved numerically at steady state for a certain fixed value for the specific input used in the figure. The other inputs are fixed at their nominal values listed in Table 1. The process states are set free during the numerical solution. The procedure is repeated to cover the input range shown in each figure. It should be noted that the figures show the plot for only six process states namely; W_D , B_D , T_{B0} , T_{B1} , L_{B1} and L_{B22} for simplicity and because they are the most critical ones. Our work focuses on the brine level instead of the distillate level because the former is well known of creating operational problems such as shut down or frequent adjustment of the orifice opening. In all steady state simulations, the plant is considered to operate in open-loop fashion, i.e. no control loop is used except for the steam temperature. In fact, the low-pressure steam used in the brine heater is supplied at 120 °C. However, in common MSF plants, the steam temperature entering the brine heater is regulated via manipulating a condensate recycle stream. Therefore, we consider that T_s can be perfectly adjusted to the desired temperature via an external control loop. In the numerical solution, this situation is emphasized by letting T_s to vary freely. It should be noted also that the process model is linearized and the eigen-values are computed at each steady state solution point. The computed eigenvalues are used to check the stability mode of the process at each specific steady state point. Therefore, a solid line will be used in the figures if the system is stable or a dashed line otherwise.

Figure 3 shows the effect of B_0 on the steady state value for the aforementioned six process key variables. Clearly, increasing the recycle brine flow has an adverse effect on the distillate product. High brine flow at fixed amount of steam reduces T_{B0} and consequently the subsequent T_B 's. As a result the rate of evaporation reduces producing less distillate. Moreover, the reduced evaporation rate leads to buildup in the brine level especially at the first flashing stage as clearly

shown in the figure. As brine flow is reduced, the top brine temperature increases leading to higher distillate production. The distillate production reaches a maximum value then starts falling as B_0 is decreased further. Generally, it can be concluded that lower recycle flow is economically favorable. However, part of the upper values for W_D , which corresponds to lower values for B_0 is not achievable since it requires higher T_{B0} . The latter is outside of the controllability region because the maximum allowable steam temperature is 120 °C. Specifically, the lowest admissible value for B_0 is around 141 ton/min at which $T_{B0} = 118$ °C and $W_D = 19.3$ ton/min. As far as the level stability is concerned, variation of B_0 exhibits considerable effect on the level of the upstream stages, but a minor effect on the last stage level.

Figure 4 shows the effect of W_F on the steady state value for the process key variables. The seawater feed rate affects the energy balance of the reject stages and the mass balance of the last stage. Obviously, variation of W_F has a little effect on the top brine temperature and distillate production rate. This is because the thermal effect of W_F is limited to the energy balance of the condenser tubes in the rejection section. Consequently, minor effect on the brine level of the upstream stages is observed as shown by the plot of L_1 . On the other hand, higher value for W_F increases the makeup flow, which in turn affects the mass balance of the last stage substantially leading to large buildup in the brine level. The opposite is also true. As a conclusion, W_F has a minor effect on the process economy, but a serious impact on the stability of the brine level in the last flashing stage. Similarly Figure 5 depicts the impact of varying the reject flow on the process steady state behavior. The reject flow has the same serious effect of W_F on the mass balance of the last stage, but on the opposite direction. For example, when Rej increases, the makeup flow decreases causing a large drop in the brine level at the last stage. On the other hand, the thermal effect of Rej on the process is much less than that of W_F . The reject flow simply disturbs the energy balance of the last stage through altering the makeup flow, which is then transmitted to the other stage through the temperature of B_0 . Therefore, variation of the reject flow has no economical benefit, but rather detrimental effect on the brine level of the last stage.

Figure 6 illustrates the process behavior for variation in the seawater feed temperature. Obviously, higher T_F will increase the condenser temperature in the reject section and consequently the brine temperature in the recovery section via the

temperature of the recycle brine flow. The result is a smaller overall temperature drop because the temperature of each stage becomes close to each other. Therefore, the overall evaporation rate and thus the distillate product is less. Higher feed temperature also affects the brine level of the last stage. Figure 7 demonstrates the steady state simulation resulted for variation in the steam flow rate. It is clear that W_s has an apparent thermal effect. As W_s increases, T_{B0} also increases and so the brine temperature of all stages. This behavior produces more vaporization and distillate product. It is evident therefore that W_s is a crucial parameter for the process economy. Note that, as observed earlier, higher vaporization rate is associated with reduction in the brine level. The difference here is that the brine level of all stages is affected.

The above steady state analysis for the fully open-loop process revealed some general guidelines on how to efficiently utilize the process inputs. First, the variation of W_F and Re_j flow rates have no economical benefit, but serious effect on the brine holdup in the last stage especially at their extreme values. Therefore, it is recommended that they should be kept constant. Secondly, the seawater feed temperature possesses negative effect on the process economy especially at high values. However, keeping T_F at low temperature requires additional resources and thus increases operational cost especially in summer. Accordingly it is recommended to keep T_F constant. On the other hand, the simulated results indicated that B_0 and W_s seem to be the key parameters for optimizing the process operation. Hence, they can be manipulated to achieve desired economical operation. It should be mentioned though that low B_0 flow leads to low brine height in the first stage, which should be avoided because it may cause blow through situation. The stability analysis also indicated that the open-loop MSF process is internally stable at all operating conditions as indicated by the solid line shown in Figs. 3-7. Moreover, pictorial of the poles of the process model at the nominal operating conditions is shown in Figure 8. It is clear that all poles are located at the RHP. Interestingly, the poles are symmetric due to the symmetry of the Jacobian matrix.

To illustrate the detrimental effect of W_F or Re_j on the stability of the brine level, the above steady state analysis is repeated with the blow-down being controlled at fixed value. In practice regulation of B_D is achieved through manipulating its pump speed. Figure 9 shows the result of the static simulation for possible range of W_F . As

the figure illustrates, at low W_F flow rate there is no sufficient liquid hold up to maintain the required fixed B_D flow rate. This phenomenon is clear since the liquid level in the last stage becomes negative. Physically, negative values for the level is meaningless, however it is numerically possible and manifests total dry out. Similarly, dry out in the last stage occurs at high Re_j flow rate. The simulation result for this case is not shown here for simplicity. The stability analysis indicates that the process operates in an unstable mode at all operating conditions shown in the Fig. 9. A dashed line is used intentionally in the figure to highlight the instability. The poles for the process model when the blow-down is controlled are shown in Figure 10. The figure shows at least four positive poles. The instability analysis indicates that controlling the blow-down instead of the level at the last stage is a bad experience. This finding is not surprising. It is well known that storage tank with fixed outlet flow rate operates as an integrator system.

Closed-loop simulation:

It is more interesting though to study the steady state behavior when the process is under control, which resembles the realistic operation of an MSF process. Specifically, the W_s - T_{B0} and B_D - L_{B22} loops will be closed. This means the top brine temperature is controlled via the steam flow and the last stage level via the blow-down flow. The set points for T_{B0} and L_{B22} at the operating condition given in Table 1 are around 93 °C and 0.56 m, respectively. These loops are considered here because they simulate common industrial practice and they stand as the most crucial ones. In the following figures, T_{B22} will be shown instead of T_{B1} . According to Figs. 3-7, T_{B1} showed identical trend to that of T_{B0} and very small difference in magnitude. This explains the reason for substituting T_{B22} with T_{B1} in the figures. Figure 11 illustrates the values of the process key variables at steady state for a given range for B_0 . The figure shows fixed value for L_{B22} and T_{B0} because they are under control. For this reason as B_0 increases W_s was also increased to maintain the top brine temperature at its set point. Also B_D had to vary to maintain L_{B22} at the set point. Interestingly, higher recycle brine flow is in favor for higher distillate product. This is in contrast to the finding reported in Figure 3 for open-loop operation. The higher B_0 , the higher the efficiency of the condenser tube is. Since T_{B0} is fixed, the subsequent T_B 's are kept at high values. This situation of high efficiency and high T_B enhances the vaporization and condensation rates producing more distillate product. This finding explains the

reason for using B_0 to maximize W_D in the industrial practice. It should be pointed though that the growth in production rate demands more steam, which lowers the performance ratio.

The impact of W_F and Rej flow rates on the process under control is shown in Figs. 12 and 13. As discussed earlier, both inputs have weak thermal effect, which even becomes much weaker when T_{B0} is under control. However, their detrimental effect on the last stage level is clearer here. Since the level is controlled, the influence of W_F and Rej is conveyed to the blow-down flow. This is manifested through the very large or negative values for B_D . The negative value for B_D , physically indicates complete shut down of the brine outlet, which is necessary at low W_F or high Rej to maintain the level at its set point. The possibility of shutting B_D off or setting B_D at maximum is expected when the plant throughput decreases or increases and L_{B22} is fixed. Due to the fact that the maximum allowable B_D flow is restricted by the plant design, i.e. pump capacity or orifice maximum opening, the last stage is vulnerable to flooding.

Lastly, Figure 14 depicts how the process states respond to changes in T_F at steady state while T_{B0} and L_{B22} are controlled. In this case, T_F delivered the same effect observed in Figure 6, i.e. when the process operates in an open-loop fashion. As discussed earlier T_F has a strong thermal effect. As a result, T_{B22} increases substantially with increasing T_F . Therefore, the overall brine temperature drop, i.e. $T_{B0}-T_{B22}$, is reduced bearing in mind that T_{B0} is fixed. Moreover, as T_F increases the subsequent condenser temperatures (T_C 's) increase and their values get closer to each other and to T_{B0} . For these two reasons the vaporization efficiency is degraded leading to a smaller distillate production. However, since T_{C1} becomes closer to T_{B0} , the required steam lessens as shown in Figure 14, which improves the performance ratio. Therefore, to retrieve the MSF thermal efficiency during summer time the feed temperature should be cooled down or the set point for the top brine temperature should be raised. The latter is the common practice in industrial application. As mentioned earlier, higher T_F minimizes the steam consumption. On the other hand, decreasing T_F will result in positive effect on the total distillation rate. Note that since T_{B0} is controlled the brine temperature in subsequence flashing units will remain

relatively high. However, the low feed temperature will reduce the temperature in the condenser tubes. This situation leads to higher vaporization rate and consequently production rate.

The above steady state analysis with T_{B0} and L_{B22} under control presented significant MSF process performance with respect to its inputs. The seawater feed flow and the Reject flow continued to deliver the same thermal and material effect observed when the process is operating in fully open-loop mode. The exceptions are, smaller thermal effect because the top brine temperature is fixed and more apparent material effect on the last stage level. The latter indicated that at extreme values for W_F or Rej , the desired level may not be maintained without deriving the Blow-down flow to its constraints. Similarly, B_0 and T_F provided the same strong thermal effect. For the case of B_0 , the thermal effect is in the opposite direction to that observed in the open-loop case. The closed-loop results showed higher distillate production rate and steam consumption at high recycle flow, and lower distillate production rate and steam consumption at high feed temperature. As far as the level operation is concerned, all the four inputs still influence the brine level even if the last one is controlled. For example, B_0 and T_F still affect the brine level of all stages except the last. Similarly, W_F and Rej affect the blow-down flow, and if the latter set point is not selected properly undesirable operation may occur. As far as the internal stability is concerned, the system eigenvalues are examined and the process is found internally stable as proven by the negative poles shown in Figure 15 and emphasized by the solid line used in Figs. 11-14. This means that the brine level does not runaway spontaneously, rather it may reside at unfavorable high or low values depending on the process conditions.

Generally, the previous open-loop and closed-loop steady state tests illustrates the effect of a single input at a time. It is more informative to examine the combined effect of more than one variable. T_{B0} and L_{B22} will remain under control. Since T_{B0} is controlled, the influence of steam flow and temperature can be excluded. Thus, only four input variables are left namely, B_0 , W_F , T_F and Rej . Because the combined simultaneous effect of three variables is difficult to visualize graphically, only the simultaneous effect of two inputs at a time will be shown. Figure 16 shows the combinatorial effect of B_0 and W_F on the process behavior. The process variables, i.e.

L_{B1} , W_D , W_S , and B_D , are found to respond monotonically and linearly to both inputs with B_0 having the largest effect and W_F negligible effect. The resulted trends are in agreement with that obtained for each individual input. Slight non-linearity is observed for W_D reaction at high B_0 values. The obtained trends are not seriously influenced by the combined effect except at high B_0 and low W_F where negative blow-down is obtained. As figure 16 demonstrates, the performance ratio responds nonlinearly to variation in B_0 and it reaches its maximum value at low brine recycle flow. The seawater feed flow showed minor effect as expected from the earlier investigations. Figure 17 depicts the combinatorial effect of B_0 and T_F on the process variables. The combined effect shows almost monotonic and linear response following the same trends concluded from the previous trends for individual inputs. Unlike the results obtained in Figure 16, the process variables vary with both inputs, i.e. B_0 and T_F . Interesting results are obtained for the performance ratio manifested by the concave plane surface shown in Figure 17. In this case, the maximum performance ratio occurs at high B_0 and an intermediate value for T_F .

Overall, figures 16 and 17 do not exhibit notable nonlinear behavior as expected from the simultaneous variation of two inputs. As a result, the same previous general guidelines obtained for the single-variable steady state analysis can be also applied to two-variables steady state analysis as follows. Higher B_0 benefits the distillate production, but consumes more steam and brings the level to a high value. Variation of W_F has a marginal effect on the distillate production, but a serious effect on B_D . Thus extreme values for W_F should be avoided. Perturbation in T_F has a clear influence on the production rate and on the brine level. Similar analysis was carried out for the combined effect of B_0 and Re_j on the process behavior. However, the results are excluded here because they show no significant complexity or nonlinearity behavior. Moreover, the results almost similar to those for W_F .

Process optimization

It is clear from the steady state analysis presented that several process parameters have different effect on the distillate production rate and on the steam consumption rate. Moreover, the effect of these parameters is overlapping. It is also found that increasing the distillate production rate may require additional steam consumption, accordingly trade-off situation exists. In this section, the optimum

operating condition that maximizes the performance ratio is formulated and solved. The MSF process in hand has 68 states covering the brine temperature, condenser temperature, brine level, distillate level for the last stage and the brine top temperature. In addition, the process has 6 operation parameters (process inputs), which are the seawater feed flow, W_F , feed temperature T_F , the reject flow, Rej , recycle brine flow, B_0 , Steam Flow, W_s , and the Steam temperature T_s . The optimization problem can be formulated as follows:

$$\max_{X,U} PR = W_D / W_s$$

subject to:

$$X^l \leq X \leq X^u$$

$$U^l \leq U \leq U^u$$

$$h_i = f_i(X,U) = 0, \quad i = 1, \dots, 68$$

$$g = Rej - W_F \leq 0$$

where X is the vector space for the plant states, i.e. $X = [L_1, \dots, L_{22}, T_{B1}, \dots, T_{B22}, T_{C1}, \dots, T_{C22}, L_{D1}, T_{B0}]$ and U is the vector space for the plant operation parameters (inputs), i.e. $U = [W_F, T_F, Rej, B_0, W_s, T_s]$. The superscript l and u indicates the admissible lower and upper values for the states or inputs. The bounds on the process inputs can be determined from the existing plant specifications. The bounds on the states can be chosen arbitrary or carefully to satisfy certain requirements. For example, specific values can be selected for the bounds on the brine level states to avoid blow-through or flooding situations. The selected values for the state and input bounds are given in Table 2. In general, incorporation of the physical bounds is important to ensure that the optimal operation lies in the feasible region of the plant. The set of equality equations, h_i , represents the mass and energy balances describing the MSF model. The equality constraints are added to ensure that the optimum condition obeys the mass and energy conservation laws, i.e. corresponds to a virtual steady state. The inequality constraint is added to guarantee positive makeup flow, i.e. the seawater flow should be greater than the reject flow. The optimization problem is solved in an open-loop mode, i.e. no control loop is in service. Solving the above optimization problem using the initial conditions given in Table 1 and the upper and

lower bounds given in Table 2, the optimum operating condition is found as listed in Table 2. It is clear that the optimum condition is almost the same as the initial condition, which is the one used industrially.

In practice, the plant may operate at different loads, therefore it is interesting to define the optimum condition for a certain range of steam consumption rate. For example, Figure 18 shows the optimum performance condition at different values for the steam flow rate in the range of [2000,3000] kg/min. The Figure is created through solving the optimization problem repeatedly at different fixed values for the steam flow rate. It is obvious that all process variables react linearly and within reasonable plant capacity over the given range for W_s . Moreover, the brine and distillate levels are within acceptable values, i.e. no signs of blow-through or flooding is observed. The results reported in Figure 18 can be utilized to determine the achievable optimum performance ratio and the corresponding values of the plant inputs and states for any value for W_s in the given range. In addition, the corresponding set points for the brine and distillate levels at the last stage can be selected. The determination of the level set points is crucial to fix the blow down and distillate flows because the latter are used in practice as manipulated variables to control the levels. Moreover, the numerical values for the levels that correspond to the optimum condition are not known beforehand. In the absence of such knowledge, the set point for the levels is normally selected arbitrary. In this way, improper selection of the set point for the distillate level may not necessarily operate the distillate flow at the desired value.

Usually, the seawater feed temperature is fixed in some MSF plants by recirculating some of the reject flow. Hence, the optimization problem is solved again, but at fixed value for the feed temperature. Figure 19 shows the result for $T_F = 15$ °C, which simulates winter conditions. As the figure demonstrates, good performance ratio can still be obtained for various grades of steam consumption at reasonable values for the operation parameters. Notably, less seawater feed and reject flow rates are required. Figure 20 depicts the result for $T_F = 35$ °C, which simulates the summer conditions. Obviously, higher performance ratio can be attained at warmer feed temperature. This is in contradiction to what have been observed in the steady state analysis for open-loop mode.. In that case, the distillate production decreases as the feed temperature increases. Because the steam flow is constant in that analysis, the

performance ratio thus decreases. However, in this case moving from a low temperature of 15 °C to a higher temperature of 35 °C, the performance ratio grows for the same range of steam consumption. The reason for the discrepancy between the two cases is trivial. In the first case, i.e. steady state analysis, the effect of a single process parameter is investigated while the remaining operation parameters were kept constant. In the second case, i.e. steady state optimization, the contribution of all operation parameters is investigated therefore, a global result is obtained.

Generally, the above optimization treatment can be used for supervisory control. In that case, the optimization problem can be solved online any time to update the set points for the entire plant control loops. For example, if some plant requirement is known such as fixed feed temperature and/or fixed seawater feed flow, the optimization problem can be solved again with these parameters set constant. The obtained solution is thus the maximum achievable performance ratio at that situation. The corresponding values for the other free operation parameters and states are then used as set points for the internal control loops. For instant, the obtained value of L_{B22} fixes the set point for the B_D-L_{B22} control-loop, L_{D22} fixes the set pint for the W_D-L_{D22} control-loop and T_{B0} fixes the set point for the W_s-T_{B0} control loop. The obtained value of Rej fixes the set point for the control loop relating the reject flow to its control valve. Similarly, the value of B_0 fixes the set point for the control loop relating the brine flow to its pump capacity or control valve, and T_s fixes the set point for the control loop relating the steam temperature to the steam condensate flow to the spray system.

Occasionally, the optimization goals can be revised to serve the actual needs, e.g. minimal cost, or maximal production etc. Any other known plant restrictions such as maximum temperature, chemical dosing, etc can be taken into account. Given the process model, the optimization can be solved frequently to re-evaluate the plant performance during environmental condition changes, anomalies, or modification of some parts of the plant.

Open-loop dynamic simulation

In practice, dynamics may occur in the plant due to sudden perturbation in plant parameters. Perturbation may result from manually changing the set point for

one or more controlled variable. It may also result from plant disturbances such as sudden changes in the feed condition and/or from minor failure of some physical components, i.e. pump, sensor, individual condenser etc. Therefore, even if the plant is brought to safe and optimal steady state operation, perturbation forces the plant to undergo transient behavior and because of time lag some of the process states especially the brine level may drift to a defective status.

In this section, the effect of perturbation in the operation parameters on the dynamic of the whole process is examined. This is carried out here by numerically integrating the MSF model for a specific step change in one process parameter at a time. This procedure is conducted twice, once when the plant is in an open-loop mode and then when the plant is in a closed-loop mode. In the following simulation, the dynamic response of the MSF main parameters to step changes in four inputs namely, B_0 , W_F , W_s and T_F is illustrated. The plant is considered to be at the initial steady state given in Table 1. Relatively large step changes might be used to clearly demonstrate the input effect.

Open-loop dynamic:

Figure 21 shows the plant states response to step changes in the recycle brine flow. Specifically, Figure 21(a-c) shows the response to -100 ton/min step change and Figure 21(d-f) shows the response to $+30$ ton/min step change in B_0 . This corresponds to -46% and $+14\%$ changes from the nominal condition. As expected, for negative changes in B_0 at fixed steam flow, the brine temperature of all stages increases. As shown in figure 21b, the effect of the recycle brine flow starts from the zero stage, i.e. brine heater, and then passes to the down stream stages. In due course, the top brine temperature responds instantaneously while the temperature response for the following stages is delayed and the delay increases with number of stages. The instantaneous response of T_{B0} is not true in real conditions. In practice, the change in B_0 takes place at the exit from the last stage and therefore, the distance from that location to the brine heater entrance introduces some dead time. However, this situation is not considered in the model. Figure 21b shows also that T_{B0} and T_{B1} grow beyond 120 °C, which the maximum allowable temperature for the steam. In this simulation, these temperatures were allowed to violate the upper bound for demonstration purposes. The growth of the whole stage temperatures affects the other

process states. For example, the evaporation rate increases leading to slightly higher total distillate production rate as shown in Figure 21c. Moreover, the high evaporation rate decreases the brine level as shown in Figure 4a. This reduction is transmitted from one stage to the next sequentially with apparent time delay introduced by the capacitance of each stage. However, no serious situation such as blow-through is observed. Overall, the result at steady state is in agreement with the observation obtained by the steady state analysis. The only interesting result is the dynamic of the brine level in the last stage, which demonstrated pronounced increase for some initial period. At the beginning of the step change the inflow to the last stage is remained at initial value while the total outflow is reduced due to the lowering of B_0 . This leads to build up in the brine level for that stage. The level starts decaying when the decrease in the level of upstream stages is transmitted to the last stage. This situation should be avoided because it may cause carryover of brine in the last stage. The dynamic behavior of the last stage level is reflected on the response of the blow-down flow. The latter is allowed to vary freely with the level to compensate for the mass imbalance for the last stage. Figure 21(d-f) demonstrates the response to positive change in B_0 , which delivers exactly the opposite trend to that obtained for negative change. Serious inverse response for L_{B22} is observed, however this does not present a blow-through situation because it occurs at the last stage. Also, no chance of drainage of upstream stages is expected because the system is operating in open-loop mode. Our simulations showed that step changes greater than +30 ton/min should be avoided because negative values for L_{B22} is obtained which terminates the numerical integration unsuccessfully. In reality, this means that the mass inventory of the last stage can not supply the required increase in B_0 . To achieve such large step change, the blow-down should be shut down for some period of time enough to allow the change in B_0 to be transmitted to the last stage inflow or the step change should be carried out gradually.

The dynamic response to step change of $-20\text{ }^\circ\text{C}$ and $+10\text{ }^\circ\text{C}$ in T_F is shown in Figure 22(a-c) and Figure 22(d-f), respectively. The perturbation in T_F will first affect the last stage because it enters the plant through the seawater feed flow. Consequently, the states of the last stage such as T_{B22} and L_{B22} will be the first to get influenced. This effect passes through the condenser tubes of the rejection section and is conveyed to the evaporator of the last stage through the reject flow. This change

will start affecting the states of the first stage after it passes through the condenser tubes of the recovery section. For this reason, the response of the primal states, i.e. T_B 's and L_B 's, will have larger time constant as clearly shown in Figure 22. Obviously, as shown in Figure 22b the negative change in T_F causes the brine temperature of all stages to drop by at least 10 degrees. The temperature reduction leads to less vaporization and consequently less total distillation production (Figure 22c). The lower vaporization rate is associated with asymptotic growth in the holdup in all evaporators. However, the brine holdup of all stages illustrates inverse response. Initially, the chain of condenser temperatures cools down and because the brine temperatures have not yet decreased, an appreciable condensation occurs causing more vaporization. Accordingly, a notable dip, which is more significant for downstream stages, in the brine levels occur. After some intervening period the brine temperatures start cooling down and consequently the vapor pressures decrease as well. Consequently, the evaporation rate diminishes leading to buildup in the brine mass. This sequence of high and low vaporization rate is reflected on the distillate production as the latter increases initially and then declines eventually (Fig. 22c). The same phenomenon is observed for positive change in the feed temperature but in the opposite direction as depicted in Figure 22(d-f). An increase in T_F leads to higher condenser and brine temperature, higher distillate rate and lower brine levels. The inverse response and time delay are still monitored. In both cases, the blow-down response follows that of L_{B22} because the former is allowed to vary freely with the latter. Overall, no notable operational instability in the brine level is detected.

Figure 23 illustrates the transient response of the MSF plant to ± 40 ton/min step change in the seawater feed flow. This corresponds to $\pm 28\%$ change from the nominal condition. The steady state analysis concluded that perturbation in W_F has a minor thermal effect. It is true that the feed flow affects the thermal efficiency of the condenser tube in the rejection section, but this effect seems to be insignificant. This is also evident here as the temperature responses shown in Figure 23(b,e) exhibit very marginal changes. Thus, the vaporization rate and the total distillate production are minimally influenced. Because the vaporization rate is maintained almost constant and that the seawater feed flow does not affect the mass balance of the recovery stages, the brine levels in the train of evaporators remain constant. The change in W_F alters only the brine level of the last stage via the material balance. Higher feed flow

at constant reject flow increases the makeup flow leading to higher brine level in the last stage and vice versa. In the simulation, W_F is considered to have instant effect on the makeup flow, which is not the common practice. In fact, perturbation in W_F should start affecting the makeup flow after it comes out of the last rejection stage and reaches the reject-makeup splitter point. The time delay introduced by traveling the aforementioned distance is not considered here. Apparently, altering W_F has no economical value but serious impact on the mass inventory of the last stage. This is why the feed flow is usually constant in real conditions.

Figure 24 demonstrates the open-loop response of the MSF process to ± 500 kg/min step change in the steam flow. This corresponds to $\pm 20\%$ perturbation from the nominal condition. For both cases, i.e., positive and negative changes, the steam flow shows clear thermal effect on the process. Obviously, the steam flow alters the brine-heater efficiency, which in turn modifies the top brine temperature. This effect is then transmitted sequentially from one stage to another. It is clear from Figure 24 that as the steam flow increases, the brine temperature as well as the distillate product increase and vice versa. Accordingly, the brine level ultimately decreases or increases as the brine temperature increases or decreases. Notable inverse response is observed especially for the downstream stages. Like the inverse response viewed in Figure 22, the time lag generated from the stage capacitance is the main reason for this irregular dynamic behavior. For example, at low steam flow the brine level in the first stage rises up due to reduction in flashing rate. This causes the pressure effect to be transmitted instantaneously to the following stages. Therefore, the outflow of each stage exceeds the inflow. This situation causes a sharp drop in the brine level for that stage. This drop is temporary as the level picks up when the flashing rate decreases in the downstream stages due to cooling down.

Closed-loop dynamic simulation:

The previous simulations covered the process response to step changes in the process inputs while the plant is operating in an open-loop mode. In general, the plant operates in a closed-loop mode; therefore, it is interesting to investigate the effect of these step changes when the regulatory controller is in service. Specifically, three control loops are considered in this work. In this case, the controlled variables are the top brine temperature, T_{B0} , the last stage brine level, L_{B22} , and the last stage distillate

level, L_{D22} , and the manipulated variables are the steam flow rate, W_s , the blow-down flow rate, B_D and the distillate production rate, W_D , respectively. The selection and pairing of the manipulated variables are obvious and follow the actual practice. There are other local control-loops that maintain the plant stream flows such as W_F , Rej , B_0 , W_s , B_D and W_D via regulating their corresponding valves or pumps. The transient response of these local loops is relatively fast. Therefore, their dynamics are excluded in the simulations.

The above three control loops use the conventional PI control algorithm. The PI settings for the W_s - T_{B0} loop is determined by the well-known reaction curve method along with the Coon and Cohen formula [15], which sets $k_c = 200$ and $\tau_I = 1$ minute. Determining the PI settings for the other two loops is more challenging and is not covered well in the literature. First, the reaction curve can not be used because the levels, i.e. L_{B22} & L_{D22} , respond unstably to step changes in the respective flow rates, i.e. B_D & W_D . Moreover, the two loops have strong interaction. Note that the sum of the blow-down and distillate product flow rates should obey the overall mass balance. This means that the sum of B_D and W_D should equals the makeup flow rate and if the latter is fixed, then the outlet flow rates can not be varied independently. For this reason, the level control loops are tuned via trial-and-error, which sets the PI setting for the B_D - L_{B22} loop at $k_c = -50$ and $\tau_I = 1$ and that for the W_D - L_{D22} loop at $k_c = -2$ and $\tau_I = 0.1$. Further tuning attempts to make the dynamic of either loop faster will create highly oscillating response in each loop. The design and tuning of these two loops may require additional attention, however this is out of the scope of this work. Here, the focus is on studying the effect of plant disturbances on the brine level in all stages while the process is under control. The emphasis on the brine level stems from the fact that brine level undergoes phases of undesirable operations [16].

Closed-loop dynamic:

Figure 25 demonstrates the plant performance in reaction to $\pm 14\%$ upset in the recycle brine flow occurring at time equals 10 minute from the start of the simulation. The net impact on the brine level is obvious. For example, as shown in the figure, the negative perturbation in B_0 decreases the brine level and vice versa. This behavior is explained as follows. Sudden reduction of B_0 result in immediate growth of T_{B0} ,

however since T_{B0} is controlled, the top brine temperature (Fig. 25e) and consequently the brine temperature of the subsequent flashing chambers are brought back to their nominal values. In the same time, the lowered B_0 rate reduces the brine velocity in the condenser tube reducing its thermal efficiency. This situation declines the vaporization rate. However, because the reduction in the brine flow rate is greater than the reduction in the flashing rate, the mass holdup in all stages lessens. The narrower vaporization rate affects the distillate level control loop. As figure 25 demonstrates, because the flashing rate is low, the nominal production rate can not be maintained, which leads to quick drainage of the last tray causing complete dry out as indicated by the negative value for L_{D22} . Since the latter is controlled, the production rate is reduced to bring L_{D22} back to nominal condition. As far as the brine level of the last stage is concerned, the sudden decrease in B_0 rate will make the total outlet flow rate higher than the inlet flow rate for the last chamber. This happens because the effect has not yet transmitted to the upstream stages especially to the inlet flow of the last stage due to the time lag comprised from the cascade of the flashing chambers. As a result, L_{B22} grows for some period, but eventually goes back to its nominal value because the controller regulates B_D to counteract this situation (Fig.25c,f). Interestingly, B_D settles at a new value higher than the initial one. This is off course to balance the loss in the production rate so that the overall mass balance is conserved. The same reasoning and analysis apply to the positive change in B_0 . Clearly, the response of the controlled and manipulated variables for positive and negative upsets is symmetric. This indicates that the process behaves linearly in the given range of upsets in B_0 .

Since no dead time for the recycle brine flow is considered in the model, the perturbation in B_0 affects both L_{B22} and L_{B1} immediately. The effect is then transmitted sequentially from the first stage down to the last stage. As shown in Figure 25, the time lag from one stage to another is minor, but obvious. Although the brine level varies with perturbation, no serious behavior such as carryover or blow through occurs. On the other hand, temporal flooding or dry out conditions may occur in the distillate level. The dry out is undesirable because it causes cavitation of the pump. To avoid such problems, the implementation procedure of the controller should be modified. For example, one should allow the set point for the distillate or brine level in the last stage to vary with changing operating condition. This can be

achieved by using either the distillate or brine level set point as manipulated variable to maintain the overall mass balance.

The process is simulated for $\pm 14\%$ step change in W_F . The impact of this upset on the brine level of all stages is negligible. For this reason, the simulation results are not shown. Alternatively, Figure 26 shows the process response to -20 and $+10$ °C step changes in the feed temperature. It is clear that positive change in T_F increases the condenser temperature of all subsequent stages. Because the brine temperature is kept high by controlling the top brine temperature, the temperature difference between the condenser tube and the brine pool becomes smaller. The outcome is less vaporization rate and consequently higher brine level. Exactly the opposite trend is observed for negative change in T_F . However, in both cases the brine level is not strongly influenced. On the other side, L_{D22} passes through undesirable operations of dry out and flooding. As shown in the figure, the controlled outputs are well maintained at their set points.

The perturbation in T_F affects first the condenser temperature of the last stage since it enters the plant with the seawater feed flow. The effect passes through the condenser tubes of the rejection section before it is transmitted to the brine temperature of the last stage through the makeup flow. The upset is conveyed to the condenser tubes of the recovery section and then to the first stage evaporator through the recycle brine flow. This long trip explains the slow transient response observed in Figure 26. It also explains the apparent time lag shown in Figure 26a,b. The symmetry of the process response is still observed, but with different magnitude. The difference in magnitude is due to the difference in the value of the step changes.

Figure 27 illustrates the effect of ± 10 °C step change in the steam temperature. Commonly, an upset in T_s affects the top brine temperature directly. At positive change in T_s , the disturbance can be rejected readily since T_{B0} is well controlled as shown in Figure 27e. This in turn, despite the large dip in the brine level of the first stage, minimizes the disturbance impact on the brine level. At negative change in T_s , the top brine temperature drops dramatically because the steam flow rate saturates at its upper limit. This situation leads to less evaporation rate and consequently to build

up in the brine level. This simulation revealed that disturbances in T_s while T_{B0} is well controlled can be serious especially on the first stage level and production rate.

Figure 28 depicts the process response during malfunctioning of individual condensers. Precisely, the overall heat transfer coefficient, U_s for the first, fourth and seventh stages is considered to be 30% less than the nominal value in one case and 30% higher in another case. Commonly higher value for U_s increases the condenser efficiency and thus the flashing rate. As a result, as demonstrated by figure 28 the brine level diminishes. On the other hand, lower value for U_s decreases the condenser efficiency leading to lower flashing rate and higher brine level. In both cases, the changes in the brine level are pronounced at the upstream stage, where the error occurs, and dampen at the downstream stages. It should be noted though that the level variation at the downstream stages, that follows the seventh stage, is in the opposite direction to that at the upstream stages. For example, a positive upset in U_s decreases the level in the upstream stages and increases the level in the downstream stages. The reason for this behavior is the reduction in the brine temperature. Note that as the flashing rate enlarges at the upstream stages the brine temperature decreases. Consequently the brine temperature for the downstream stages also decreases by convection. Nevertheless, since the condenser efficiency for the flash stages that follow the seventh stage is still at its nominal value, the vaporization rate diminishes. This situation raises the brine level in these stages. After all, the influence of anomalies in the heat transfer coefficient on the brine level is innocuous.

Conclusions

A validated model for an industrial MSF plant is used to study its stability and steady state performance. The stability investigation, which is based on the eigenvalues of the linearized model for the process model, revealed that the process and more specifically the brine level is internally stable. The brine level can be made unstable if the blow-down flow is fixed or controlled. However, the common industrial practice, which involves controlling the last-stage brine and distillate levels by manipulating the blow-down and distillate flow rates respectively, preserves the internally stability of the process. Nevertheless, depending on the operating condition the level may become operationally unstable even if the last stage level is controlled. For example, as demonstrated via the steady state analysis, extreme values for the

reject and/or seawater feed flows might lead to flooding or dry out in the last stage. Similarly, high recycle flow with small evaporation rate due to low steam temperature or flow may cause the level especially in the first stage to reside at an undesirable high value. The opposite situation may lead to an unfavorable low value for the level.

The steady analysis is used to examine the impact of process inputs on the economical performance of the MSF plant and on the operational stability of the brine level. It is found that the feed flow and the reject flow have a strong effect on the brine level of the last stage but marginal effect on the plant economic, i.e. Distillate production rate. Their effect on the last-stage level is eliminated when a level controller is used. The seawater feed temperature has a powerful influence on the production rate but minor influence on the brine level. The thermal effect of the feed temperature is even more notable when the top brine temperature is controlled. The steam flow delivered remarkable impact on the production rate and on the brine level of all stages. This pronounce behavior is not surprising because the steam flow has a direct and solid action on the top brine temperature and thus plays important role in the thermal efficiency of the whole process. The recycle brine flow showed considerable effect on both the production rate and the brine level in the first stage. However, the effect on the brine level weakens while the effect on the production rate propagates when the top brine temperature and the last-stage level are controlled.

The above steady state analysis can help in determining undesirable operation conditions for the brine level. These conditions can then be avoided to ensure safe and smooth plant operation. Similarly, economically desirable conditions for each process input can be determined. Utilizing these conditions, favorable operating points that maximize the distillate product can be defined. However, these conditions can only define local optimum. Moreover, trade-off between maximizing the distillate product and minimizing steam consumption exists. In addition, plant constraints such as upper steam temperature, seawater feed temperature and safe brine levels were not considered during the steady state analysis.. Therefore, it is more appealing to optimize the plant operation taken into account the aforementioned issues. Thus, a global optimum that satisfies plant constraints can be determined using constrained optimization methods, which will be covered in the second part of this research work. It should be noted that stage venting is not included in the model. It is assumed that

the stage pressure is well maintained at the desired value through perfect control of stage venting. The effect of stage venting on the process behavior can be addressed in a future work.

Numerical optimization of the process model is used to determine the optimum operating condition. The optimization can be utilized as a tool during the planning phase and even during operation. During operation, the optimization problem can be solved online to revise the plant performance when environmental regulations, market demands or managerial decision is changed. Dynamic analysis is also carried out in the open-loop and close-loop modes of operation and revealed the following findings.

Seawater feed flow, W_F has a limited effect on the distillate production rate and therefore on the economy of the plant. In this case, it should not be utilized to improve the economy of the plant, but rather be fixed at its required value set by the engineering evaluation and planning. Feed flow may cause problems for the last stage level. However, this problem is not challenging. This is because the last level is usually controlled and that disturbance in the feed flow is commonly handled by feed-forward control.

Seawater temperature, T_F has a considerable outcome on the distillate production. The feed temperature is not an operator-driven parameter, although it could be, but an environmental-driven parameter, i.e. disturbance. Moreover, an upset in T_F is associated with slow drift, which usually influence the performance of any typical controller. Therefore, T_F should be fixed at a specific value determined by the supervisory control or engineering evaluation. This value should also be revised from summer to winter. This is the common practice in the industry.

The recycle brine flow, B_0 has a notable impact on the MSF performance. It affects both the distillate production and the brine level. Since B_0 is an operator-driven parameter, it stands as a good manipulated variable for the plant. Similarly, the steam flow possesses strong impact on the brine level and on the production rate. However, W_s is usually used to control the top brine temperature. The steam temperature is found to seriously affect the plant dynamics even when T_{B_0} is

controlled. Internal disturbances such malfunctioning of the individual condensers may also influence the brine level profile but without detrimental results.

According to the above analysis, B_0 and W_s possess both overlapping and remarkable effect of the process operation. Since W_s is commonly used to regulate the top brine temperature, B_0 is the only influential variable left free for process enhancement especially during process operation. However during startup careful utilization of both B_0 and W_s should be emphasized. Overall, the brine level seems not to undergo carryover or blow-through problems as commonly known. Nevertheless, inverse response and large changes in the brine level of the last stage is observed in the open-loop operation. Fortunately, the latter is resolved when the level of the last stage is controlled. Yet, when the level controller is active dangerous response for the distillate level in the last stage is observed. This behavior needs more attention.

Nomenclature

A_B	Cross sectional area for the brine chamber, m^2
A_{HR}, A_{HC}	Heat transfer area for condenser tube at the rejection and recover sections respectively
B	Inter stage Brine flow rate, ton/min
B_o, B_D	Recycle brine and blow-down flow rates respectively, ton/min
C	Orifice contraction coefficient
C_D	Discharge coefficient for the distillate tray
C_{pC}, C_{pB}	Heat capacity for the brine in the condenser tube and flash chamber, $kJ/kg\ ^\circ C$
D	Distillate flow rate, ton/min
g	Gravitational constant
h	Orifice height
j	As index denotes stage number
K	Orifice discharge coefficient
L, L_D	Brine and distillate height respectively, m
M_C, M_{BH}	Liquid holdup for the condenser tube and brine heater respectively
N	Total number of stages
P	Vapor pressure, bar
Rej	Reject flow rate, ton/min
t	Time, min
T_o, T_F	Reference and feed temperature respectively, $^\circ C$
T_B, T_C, T_s	Brine, condenser and steam temperature respectively, $^\circ C$
T_{B0}	Top brine temperature, $^\circ C$
U	Overall heat transfer coefficient, $kJ/min\ ^\circ C\ m^2$
V	Vapor rate, ton/min
X	Salt concentration, kg/m^3
W_F, W_D	Seawater feed and distillate product flow rate respectively, ton/min
W_{mk}	Make up flow rate, ton/min
W_s	Steam flow rate, kg/min
w	Orifice width, m

Greek letters

ρ_B	Density of brine, kg/m ³
λ	Latent heat for vaporization, kJ/kg
λ_c	Latent heat for vaporization at the distillate temperature, kJ/kg
λ_s	Latent heat for steam, kJ/kg

References

1. H. Ettouney, H. El-Dessouky and I. Alatiqi, *Desalination*, 123, (1999) 55.
2. P.J. Thomas, S. Bhattacharyya, Patra, A., and Rao, G.P., *Comp. Chem. Eng.*, 22 (1998) 1515.
3. A. Woldai, Al-Gobaisi, D.M.K, Johns, A.T, Dunn, R.W., and Rao, G.P. *IDA*, 3 (1997) 181.
4. M. Bourouis, Pibouleau, L., Floquet, P., Domenech, S. and Al-Gobaisi, D.M.K, , *IDA*, 3 (1997) 167.
5. K. Al-Shayji, Liu, Y.A., *IDA*, 3 (1997) 91.
6. M.E. ElHawary, *Proceeding of DESAL' 92, Arabian Gulf Regional Water Desalination Symposium, 15-17 November, 1992, UAE.*
7. D. M. Al-Gobaisi, Hassan, A., Rao, G.P., Sattar, A., Woldai, A. and Borsani, R., *Desalination*, 97 (1994) 469.
8. A. Hussain, Woldai, A., Al-Radif, A., Kesou, A., Borsani, R., Sultan, H. and Deshpande, P. B., *Proceeding of the IDA and WRPC World Conference on Desalination and Water Treatment, Nov. 1993, Japan, III, 119.*
9. F. Bodendieck, K. Genthner, and A. Gregorzewski, *IDA*, 3 (1997) 179.
10. Kraus, H. and A. Hassan, *IDA*, 3 (1997) 151.
11. Zhang H. and S. Wang, *IDA*, 3(1997) 103.
12. Thomas, P.J., S. Bhattacharyya, A., Patra, and G.P. Rao, *Comp. Chem. Eng.*, 22(1998)1515.
13. Hussain, A., Woldai, A., Al-Radif, A., Kesou, A., Borsani, R., Sultan, H. and Deshpande, P. B., *IDA* 3(1993) 119.
14. Emad. Ali, Khilaid Alhumaizi, and Abdelhamid Ajbar, *Desalination*, 121(1), (1999) 49.
15. Stephanopoulos, G., *Chemical Process Control*, Prentic-Hall (1984).
16. D. M. Al-Gobaisi, Hassan, A., Rao, G.P., Sattar, A., Woldai, A. and Borsani, R., *Desalination*, 97 (1994) 469.

Table 1: Nominal plant conditions

W_s	T_s	B_0	W_F	Rej	T_F	W_D	B_D
(ton/min)	(°C)	(ton/min)	(ton/min)	(ton/min)	(°C)	(ton/min)	(ton/min)
2.453	98	217.35	143.816	95.35	35	19.2	29.3

Table 2: Bounds on states and inputs

<i>Variable</i>	<i>Upper value</i>	<i>Lower value</i>	<i>Optimum</i>
$L_1 \dots L_{22}$	0.15 m	2.0 m	~ 0.6 m
$T_{B1} \dots T_{B22}$	30 °C	100 °C	88.5 ~ 39.4 °C
$T_{C1} \dots T_{C22}$	30 °C	100 °C	85.8 ~ 37.3 °C
T_{B0}	90 °C	120 °C	91.4 °C
L_{D22}	0.1 m	1.0 m	0.34 m
W_s	1.0 ton/min	3.0 ton/min	2.453 ton/min
T_s	98 °C	120 °C	98.1 °C
B_0	0 ton/min	300 ton/min	217.26 ton/min
W_F	0 ton/min	200 ton/min	143.8 ton/min
Rej	0 ton/min	120 ton/min	95.3 °C
T_F	10 °C	50 °C	35 °C
B_D	---	---	29.16 ton/min
W_D	---	---	19.3 ton/min
PR	---	---	7.87

Appendix

In this section, derivation of the model for a reduced plant with three stages is presented.

Mass balance for the three evaporator units:

$$m\dot{L}_1 = B_0 - B_1 - V_1 \quad (\text{A1})$$

$$m\dot{L}_2 = B_1 - B_2 - V_2 \quad (\text{A2})$$

$$m\dot{L}_3 = B_2 - B_3 - V_3 - B_0 + W_{mk} \quad (\text{A3})$$

Energy balance for the three evaporator units:

$$mL_1 Cp_B \dot{T}_{B1} = B_0 Cp_B (T_{B0} - T_{B1}) - V_1 [\lambda_s - Cp_B (T_{B1} - T_o)] \quad (\text{A4})$$

$$mL_2 Cp_B \dot{T}_{B2} = B_1 Cp_B (T_{B1} - T_{B2}) - V_2 [\lambda_s - Cp_B (T_{B2} - T_o)] \quad (\text{A5})$$

$$mL_3 Cp_B \dot{T}_{B3} = B_2 Cp_B (T_{B2} - T_{B3}) - V_3 [\lambda_s - Cp_B (T_{B3} - T_o)] + W_{mk} Cp_B (T_{C3} - T_{B3}) \quad (\text{A6})$$

Energy balance for the condenser tubes:

$$M_C Cp_C \dot{T}_{C1} = B_0 Cp_C (T_{C2} - T_{C1}) - UA_C [T_{B1} - 0.5(T_{C1} + T_{C2})] \quad (\text{A7})$$

$$M_C Cp_C \dot{T}_{C2} = B_0 Cp_C (T_{B3} - T_{C2}) - UA_C [T_{B2} - 0.5(T_{C2} + T_{C3})] \quad (\text{A8})$$

$$M_C Cp_C \dot{T}_{C3} = W_F Cp_C (T_F - T_{C3}) - UA_C [T_{B3} - 0.5(T_{C3} + T_F)] \quad (\text{A9})$$

Assuming steady state for the temperature of the condenser tube and by simple algebraic manipulation we can show:

$$T_{C1} = (1-b)T_{B1} + b(1-b)T_{B2} + b^2T_{B3} \quad (\text{A10})$$

$$T_{C2} = (1-b)T_{B2} + bT_{B3} \quad (\text{A11})$$

$$T_{C3} = aT_F + (1-a)T_{B3} \quad (\text{A12})$$

According to Eq. (12), the top brine temperature can be estimated at steady state by:

$$T_{B0} = T_{C1} + \frac{W_s \lambda_s}{B_0 Cp_B} \equiv T_{C1} + Q \quad (\text{A13})$$

where

$$a = \frac{W_F Cp - 0.5UA}{W_F Cp + 0.5UA}$$

$$b = \frac{B_0 Cp - 0.5UA}{B_0 Cp + 0.5UA}$$

Similarly assuming steady state for the temperature of the condenser tube and using the heat transfer relations (Eqs. 5 and 10) it can be shown that:

$$V_1 = B_0 \frac{Cp_c}{\lambda} (T_{C1} - T_{C2}) \quad (\text{A14})$$

$$V_2 = B_0 \frac{Cp_c}{\lambda} (T_{C2} - T_{B3}) \quad (\text{A15})$$

$$V_3 = W_F \frac{Cp_c}{\lambda} (T_{C3} - T_o) \quad (\text{A16})$$

By substituting the definition of V as in equations (A14-16) and the definition of T_c as in Eqns. A10-12 into Eqns. A4-6, assuming steady state for the evaporator temperature and that the contribution of latent heat is greater than the sensible heat, and algebraic manipulation it can be shown that:

$$T_{B1} = \frac{B_1 B_2}{m(B_1 b + B_0(1-b))} \frac{W_s \lambda_s}{B_0 Cp} + T_F \quad (\text{A17})$$

$$T_{B2} = \frac{B_1(B_2 + m)}{m(B_1 b + B_0(1-b))} \frac{W_s \lambda_s}{B_0 Cp} + T_F \quad (\text{A18})$$

$$T_{B2} = \frac{B_1(B_2 + m) + B_0(1-b)m}{m(B_1 b + B_0(1-b))} \frac{W_s \lambda_s}{B_0 Cp} + T_F \quad (\text{A19})$$

Where $m = aW_F + (1-a)W_{mk}$. Note also that $\frac{\lambda_c}{\lambda} \approx 1$, $\frac{Cp_B}{Cp_C} \approx 1$ are assumed while deriving Eqns. A17-19.

Finally using the definition of V , T_c and T_b given in Eqns. A14-16, A10-12 and A17-19 respectively, the state equations for the brine level can be written as follows:

$$m\dot{L}_1 = B_0 - B_1 - B_0 Cp_c (1-b) / \lambda$$

$$m\dot{L}_2 = B_1 - B_2 - B_0 Cp_c (1-b) Q / (\lambda(B_1 b + B_0(1-b)))$$

$$m\dot{L}_3 = B_2 - B_3 - V_3 - B_0 + W_{mk} - W_F Cp_c (1-a) B_2 B_2 Q / (\lambda m(B_1 b + B_0(1-b)))$$

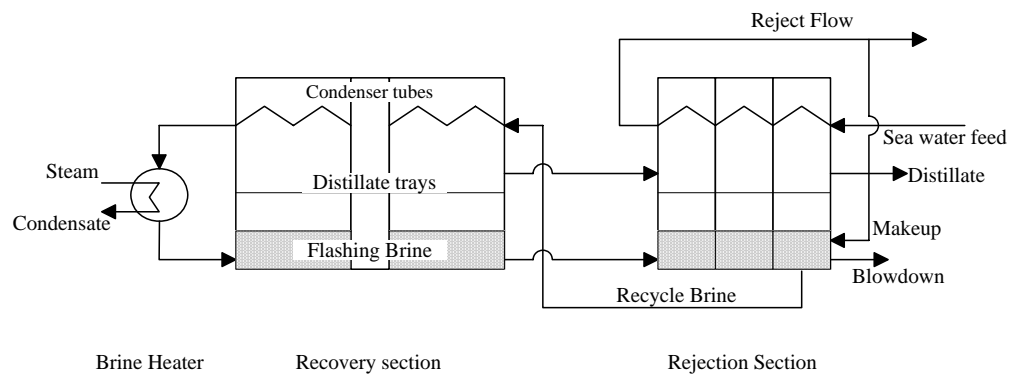


Figure 1: Schematic of industrial MSF Plant

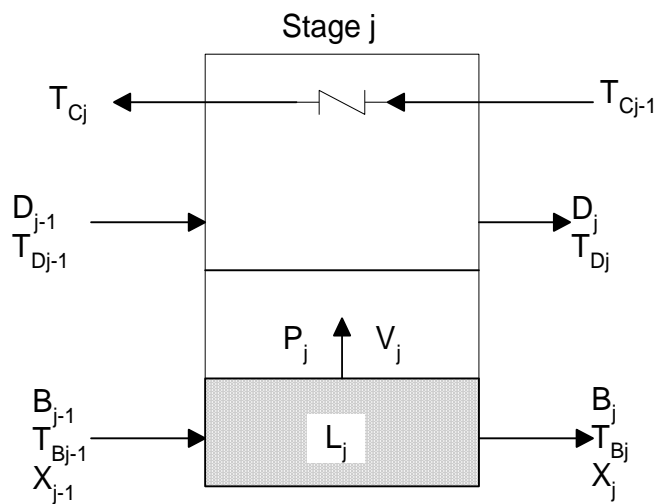


Figure 2: schematic of a single stage of a typical MSF plant

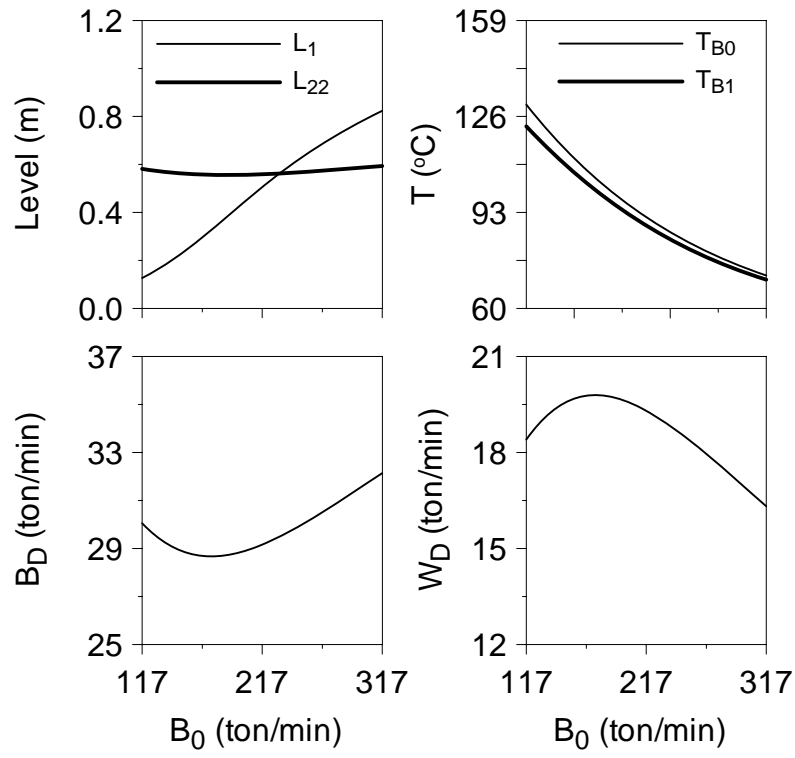


Figure 3: Effect of varying B_0 on the process steady state values in open-loop mode.

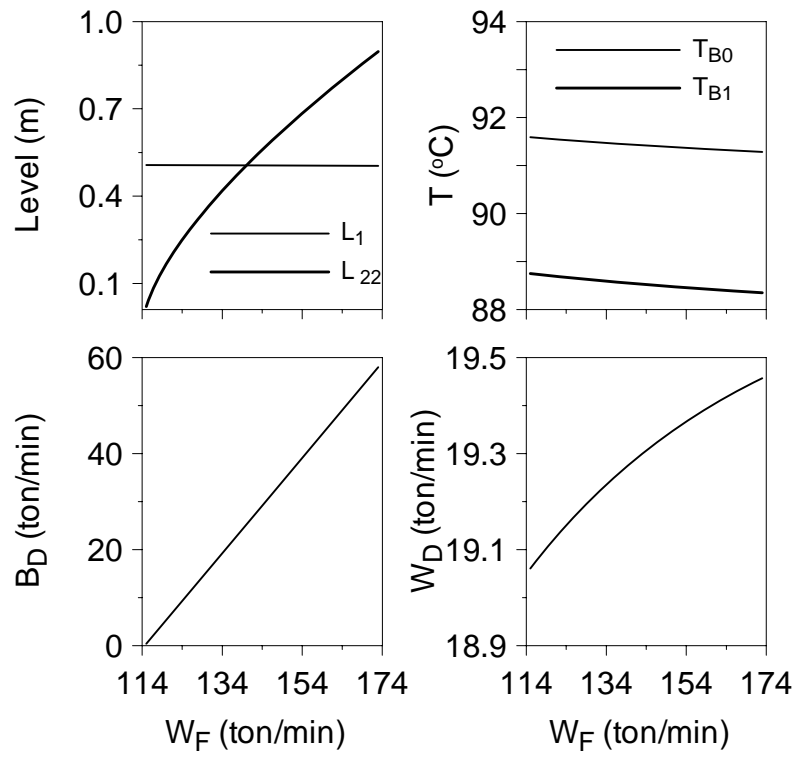


Figure 4: Effect of W_F on the process steady state values in open-loop mode.

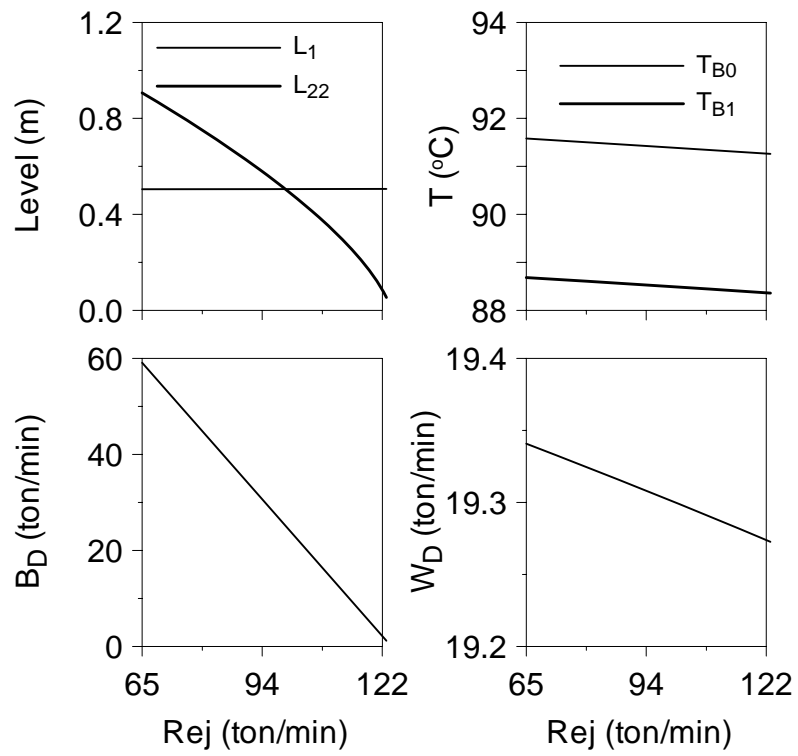


Figure 5: Effect of Rej flow on the process steady state values in open-loop mode.

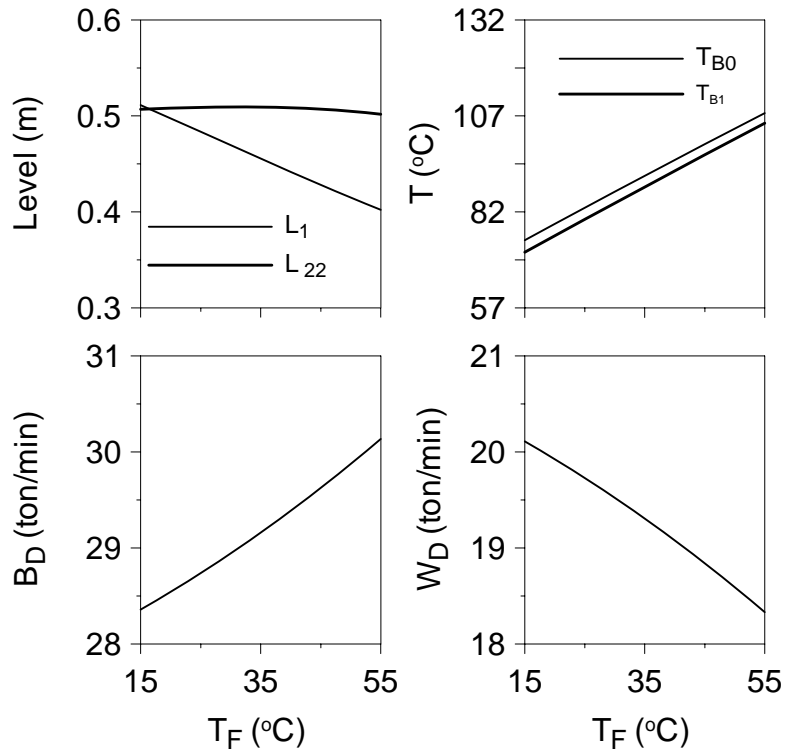


Figure 6: Effect of T_F on the process steady state values in open-loop mode.

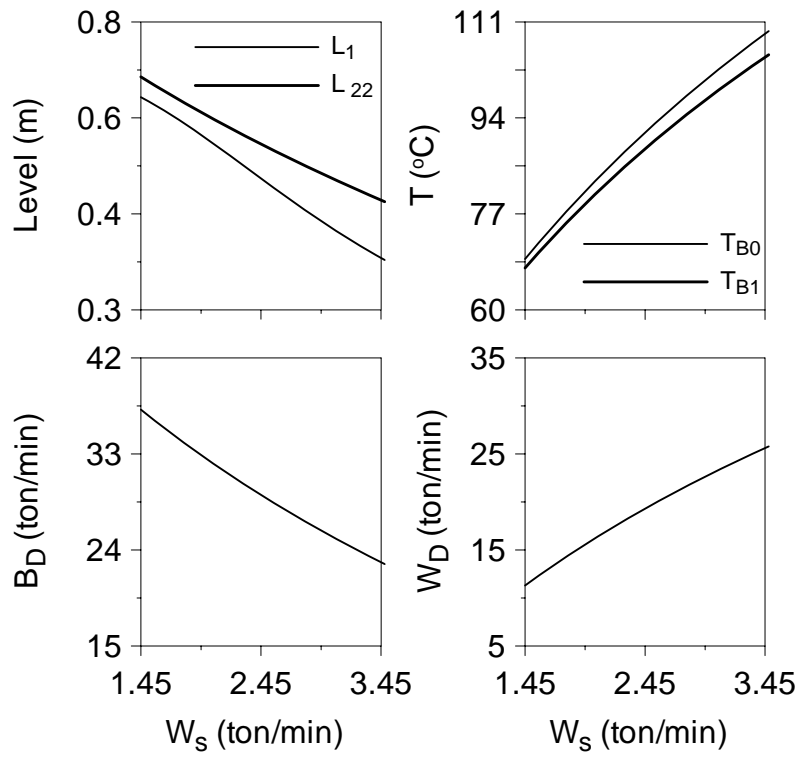


Figure 7: Effect of W_s on the process steady state values in open-loop mode.

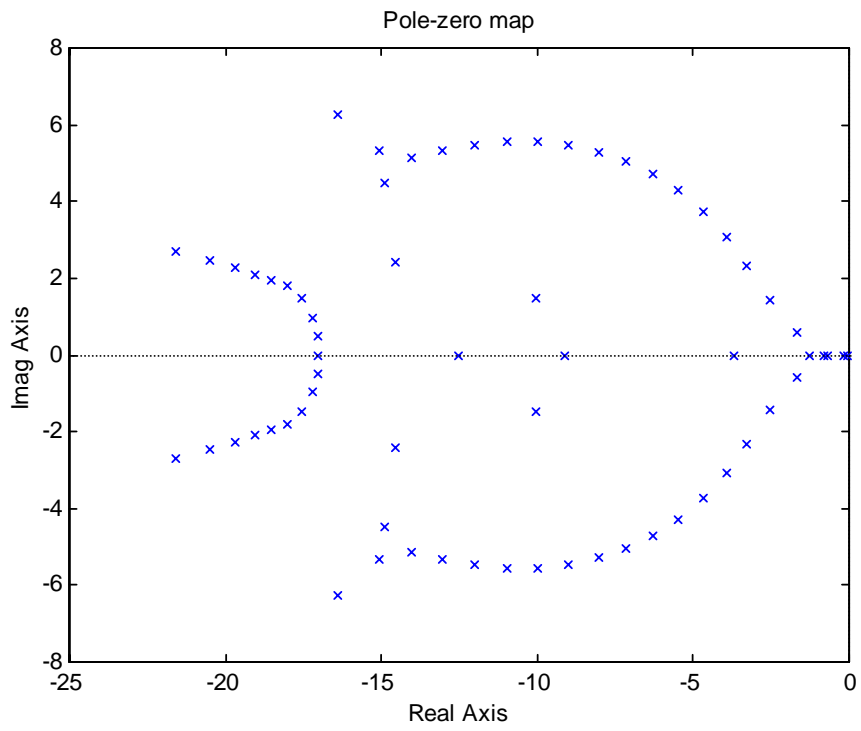


Figure 8: Poles of the process model in the open-loop mode.

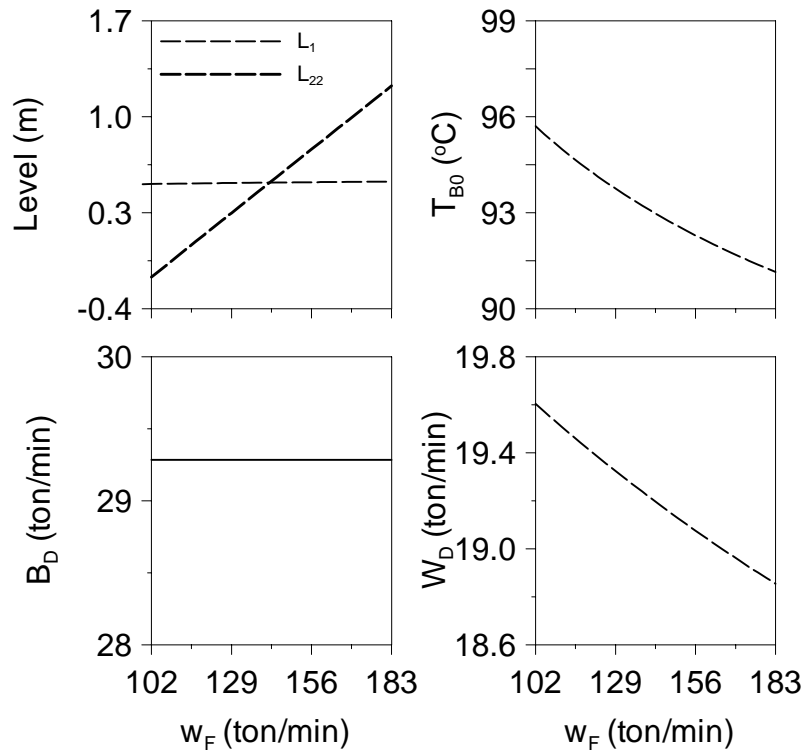


Figure 9: Effect of W_F on the process steady state values with controlled B_D .

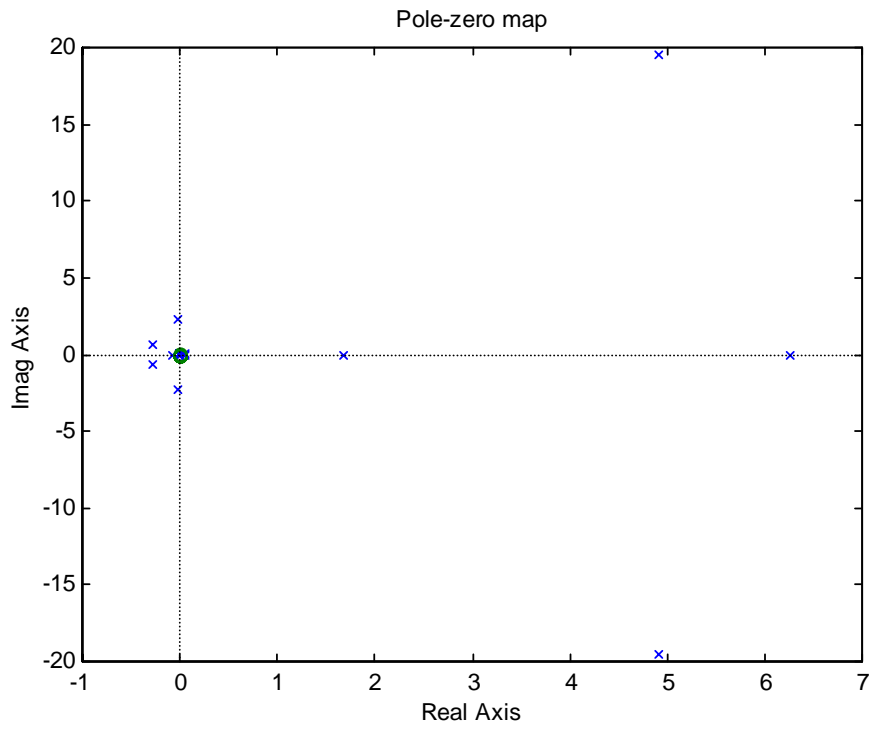


Figure 10: The poles for the process model when B_D is controlled.

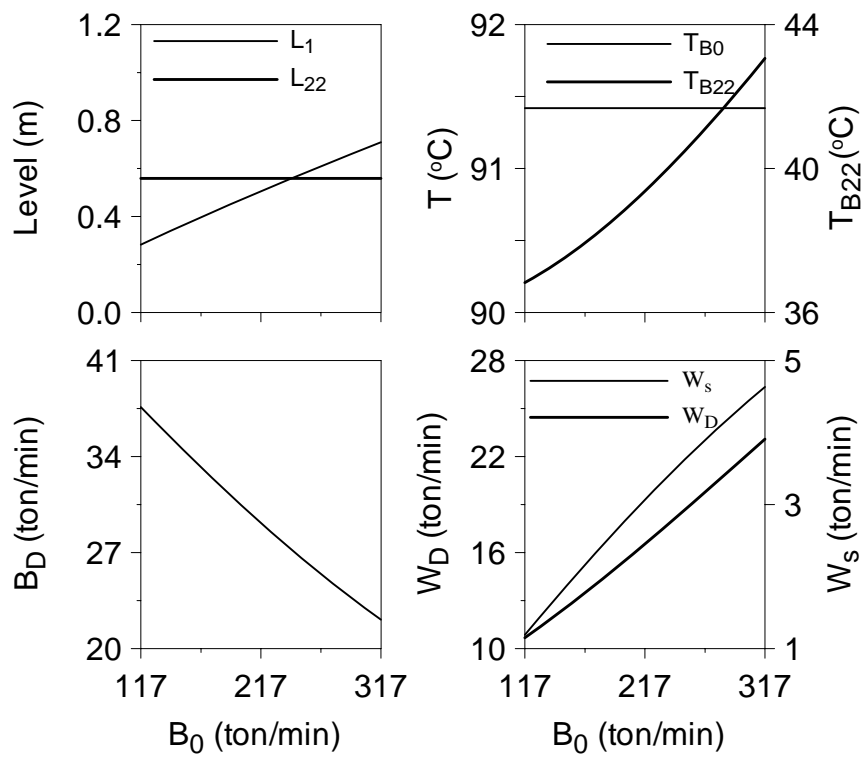


Figure 11: Effect of B_0 on the process steady state values with T_{B0} and L_{B22} are being controlled.

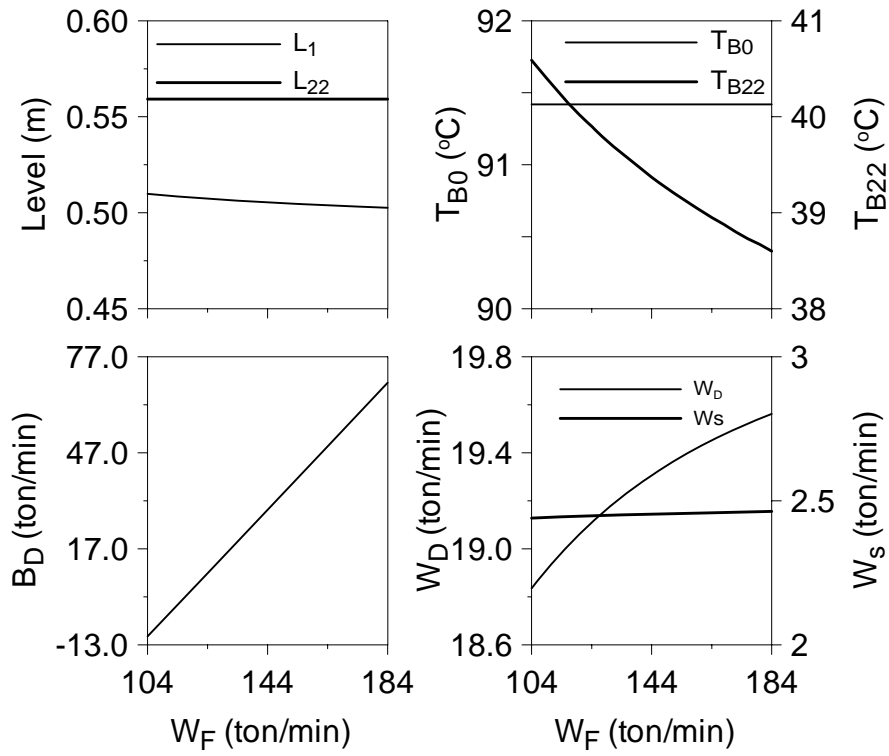


Figure 12: Effect of W_F on process steady state values with controlled T_{B0} and L_{B22} .

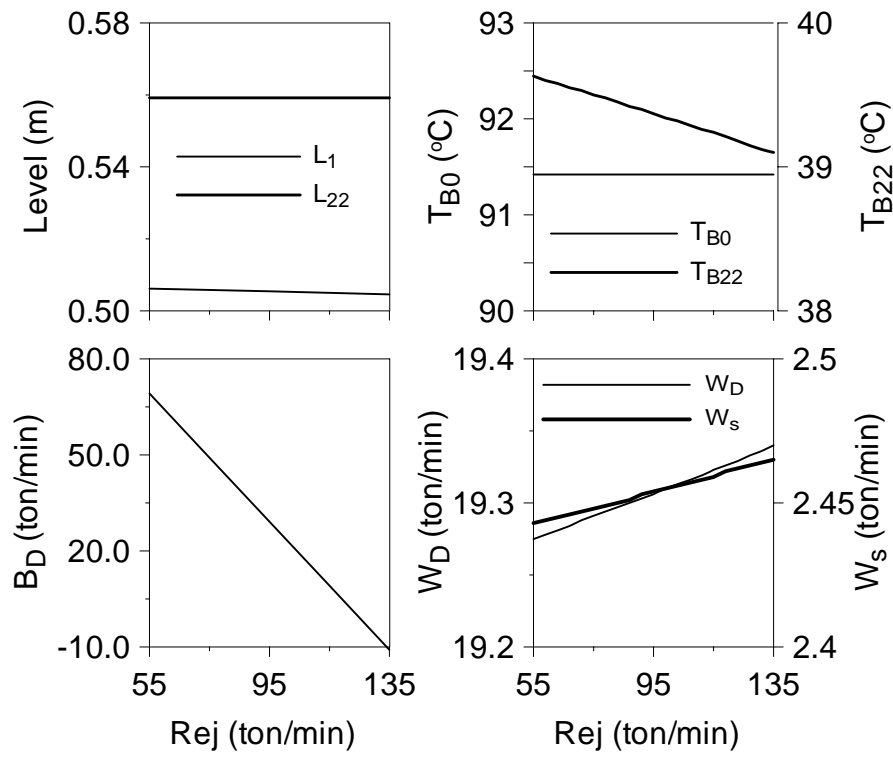


Figure 13: Effect of Rej on process steady state values with controlled T_{B0} and L_{B22} .

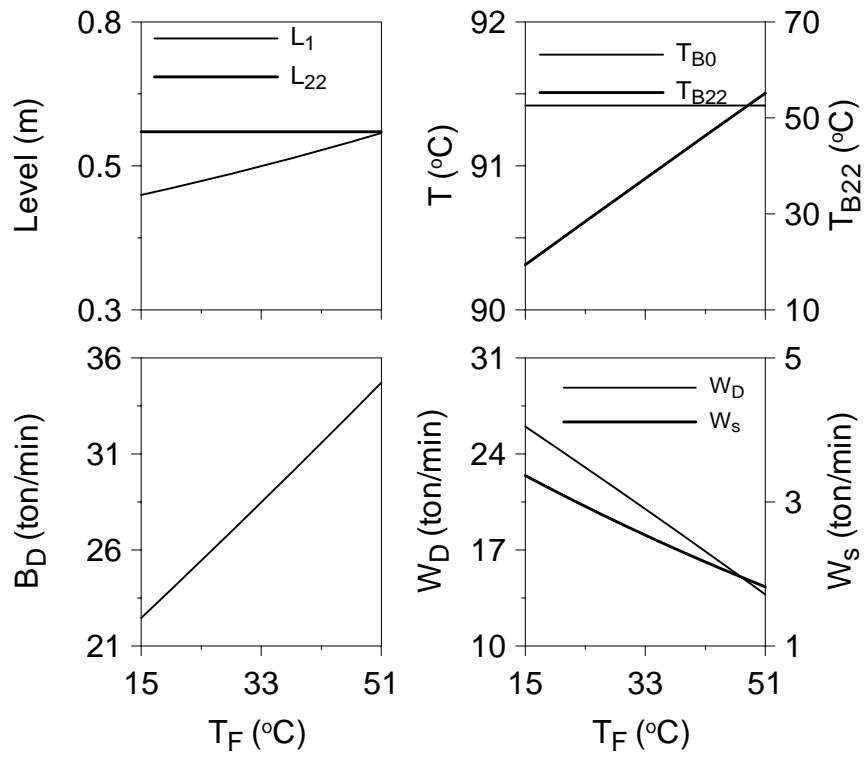


Figure 14: Effect of T_F on process steady state values with controlled T_{B0} and L_{B22} .

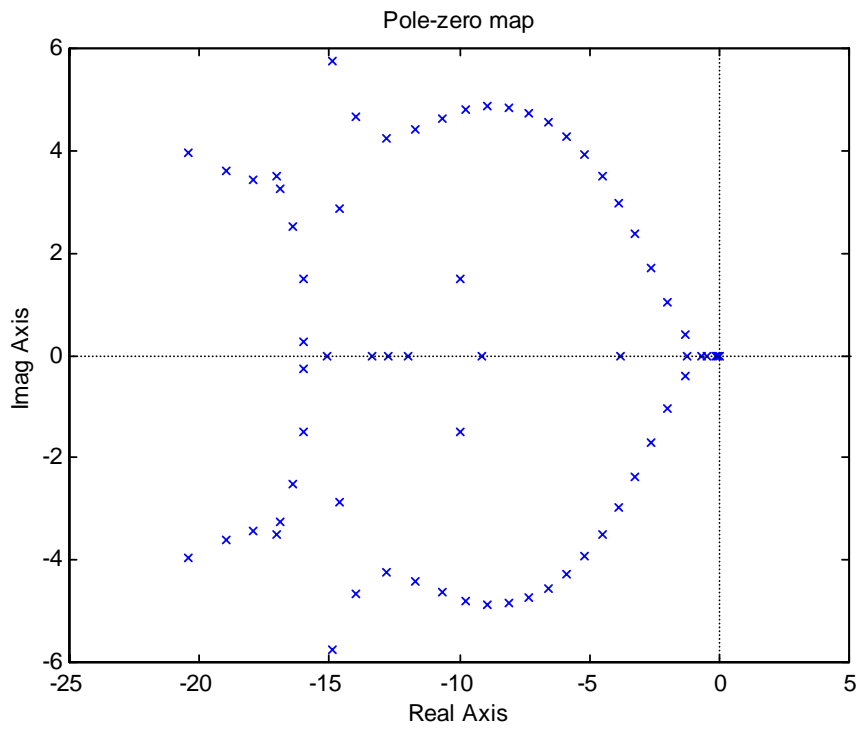


Figure 15: Poles of the process model when both T_{B0} and L_{B22} are controlled

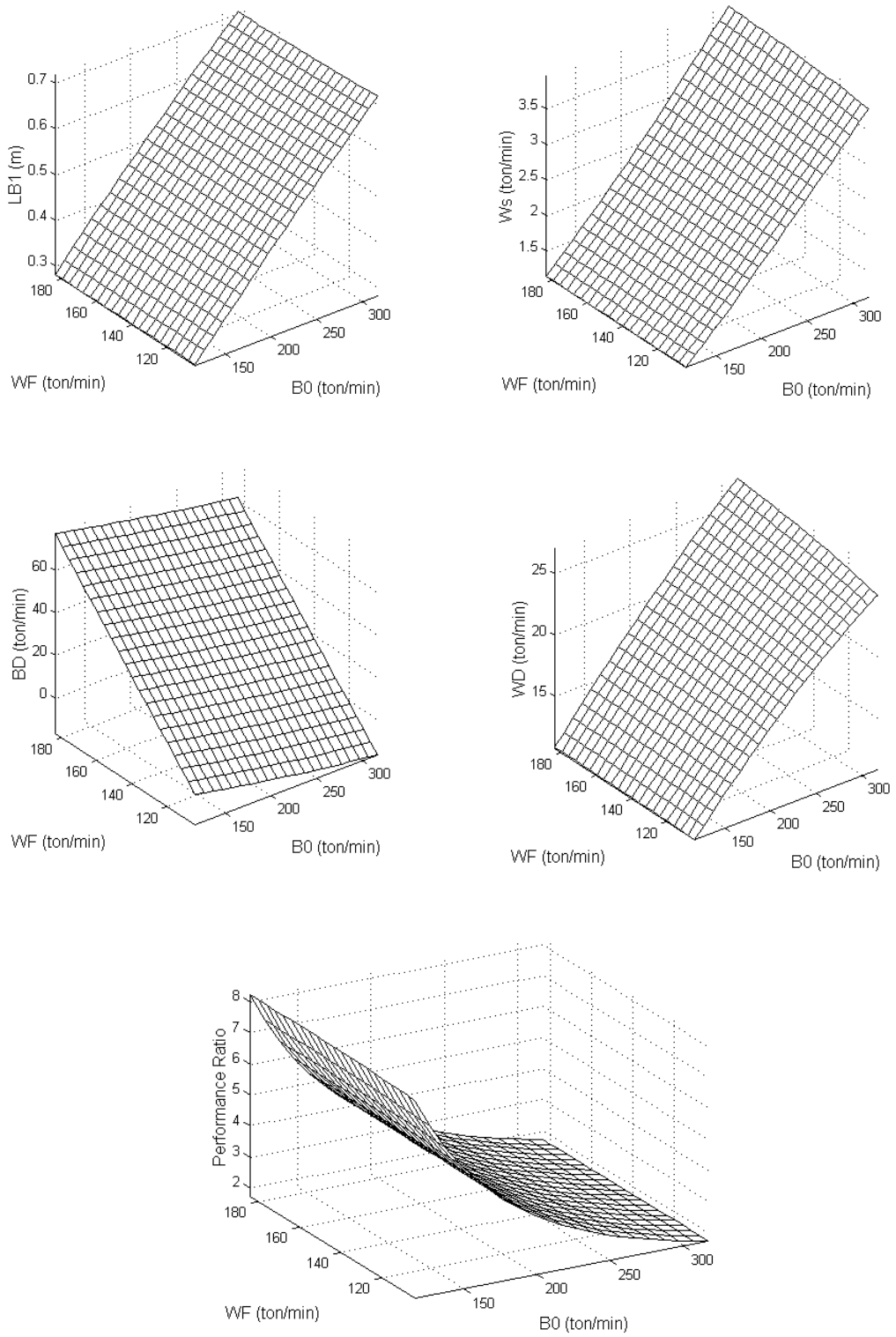


Figure 16: Combined effect of B_0 and W_F on process variables

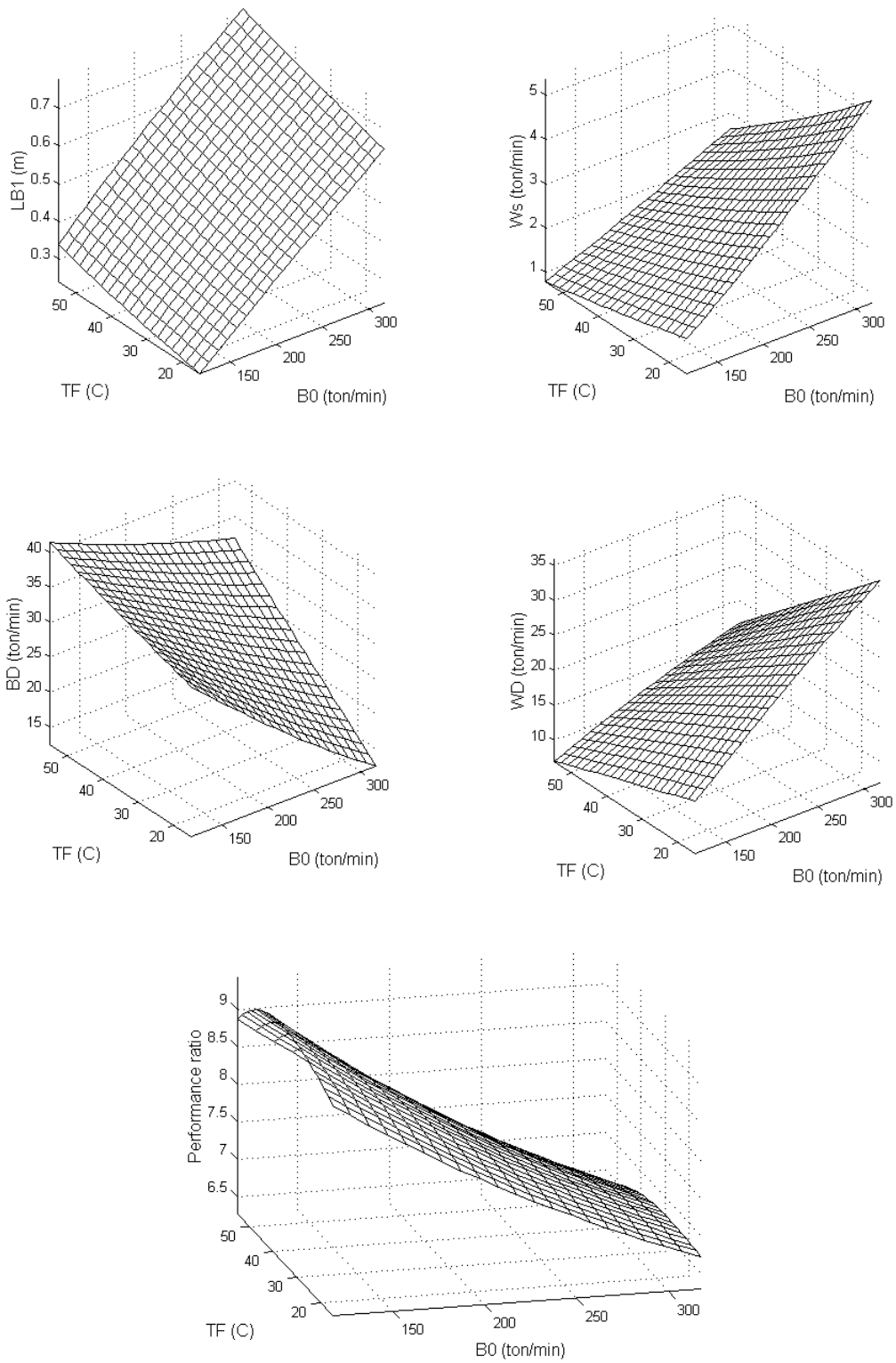


Figure 17: Combined effect of B_0 and T_F on process variables

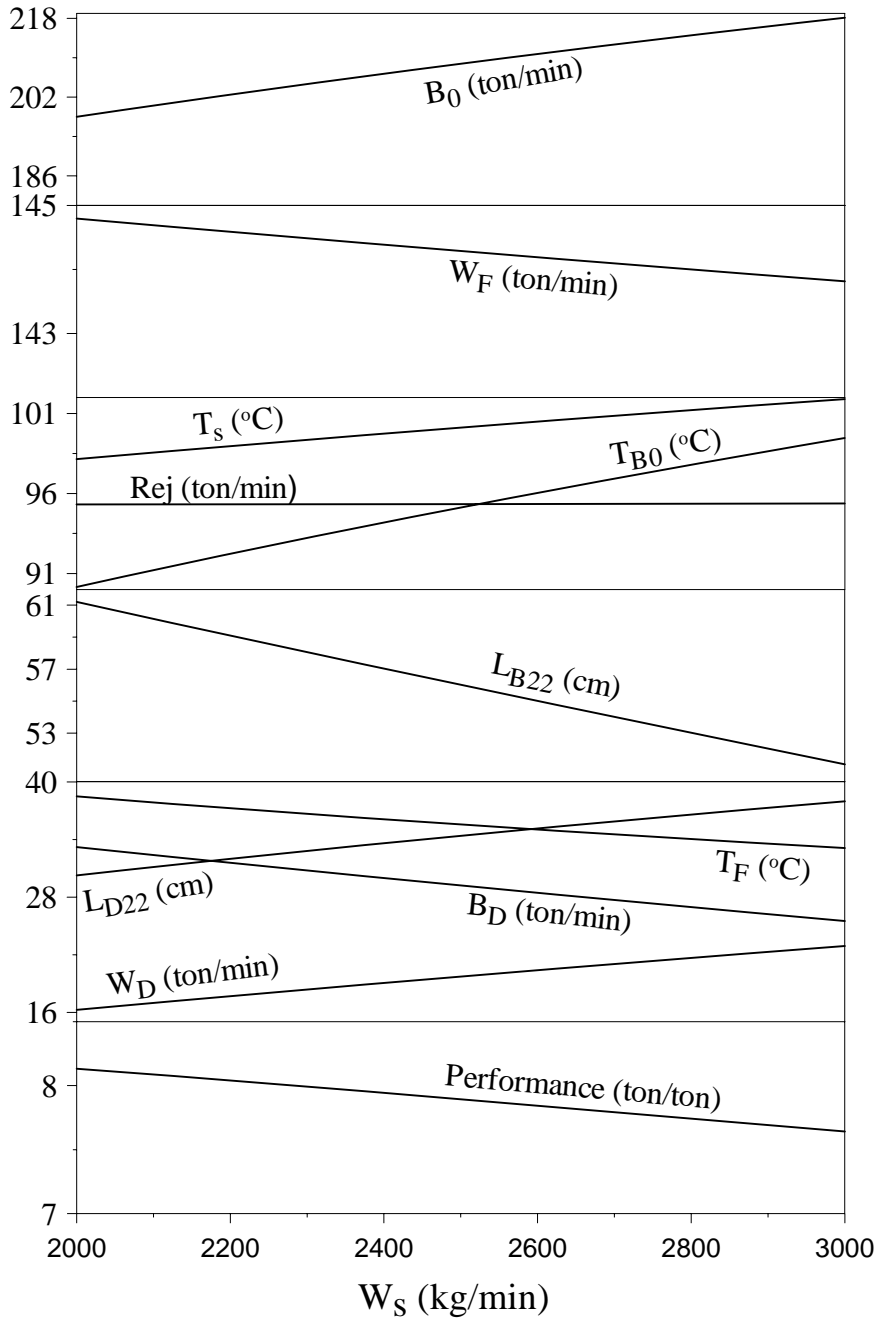


Figure 18: Optimum operating conditions for free T_F

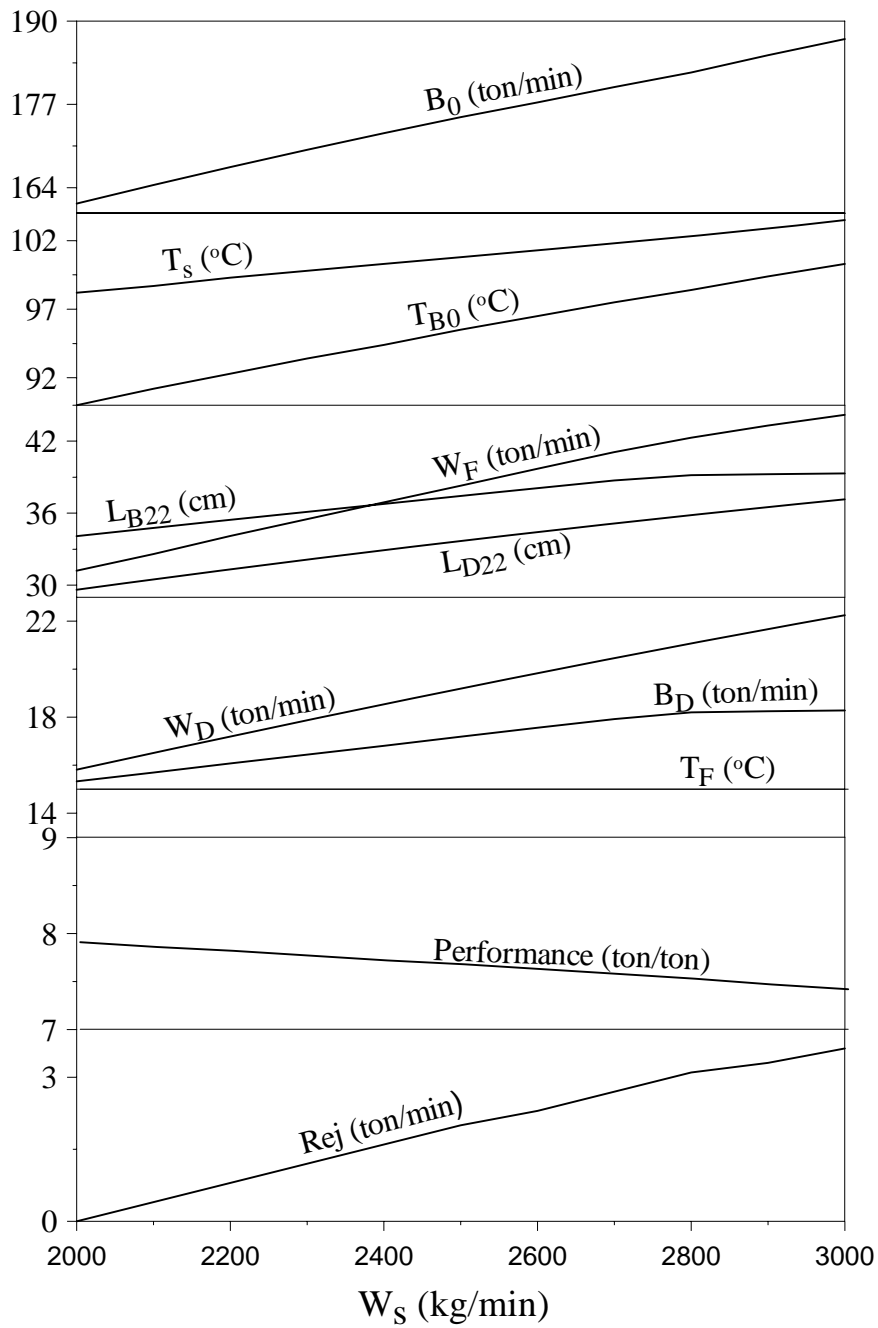


Figure 19: Optimum operating conditions for fixed T_F at 15 °C

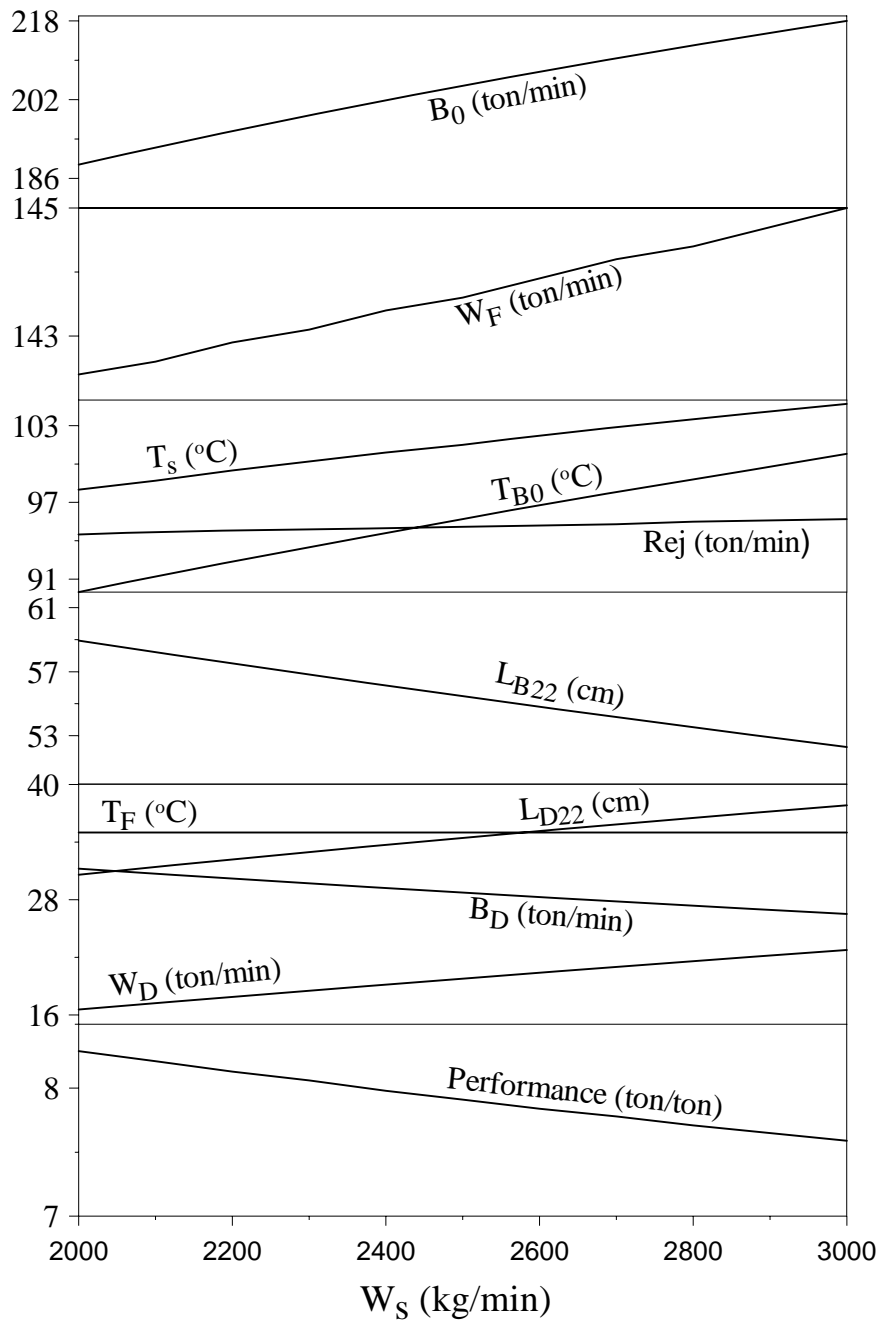


Figure 20: Optimal operating conditions at fixed $T_F = 35$ °C.

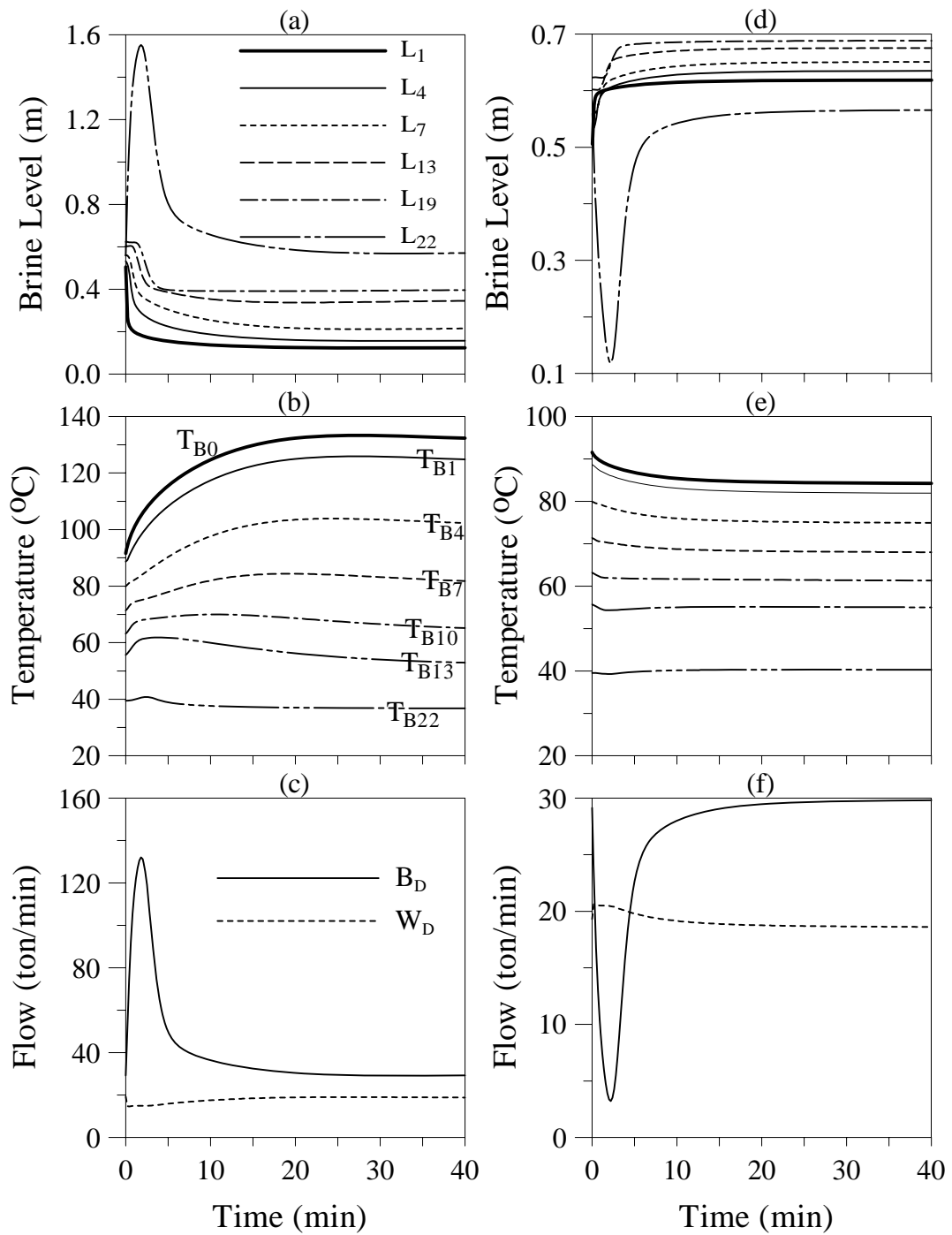


Figure 21: Dynamic response to step change in B_0 in open-loop mode, (a-c) $\Delta B_0 = -100$ ton/min; (d-f) $\Delta B_0 = +30$ ton/min

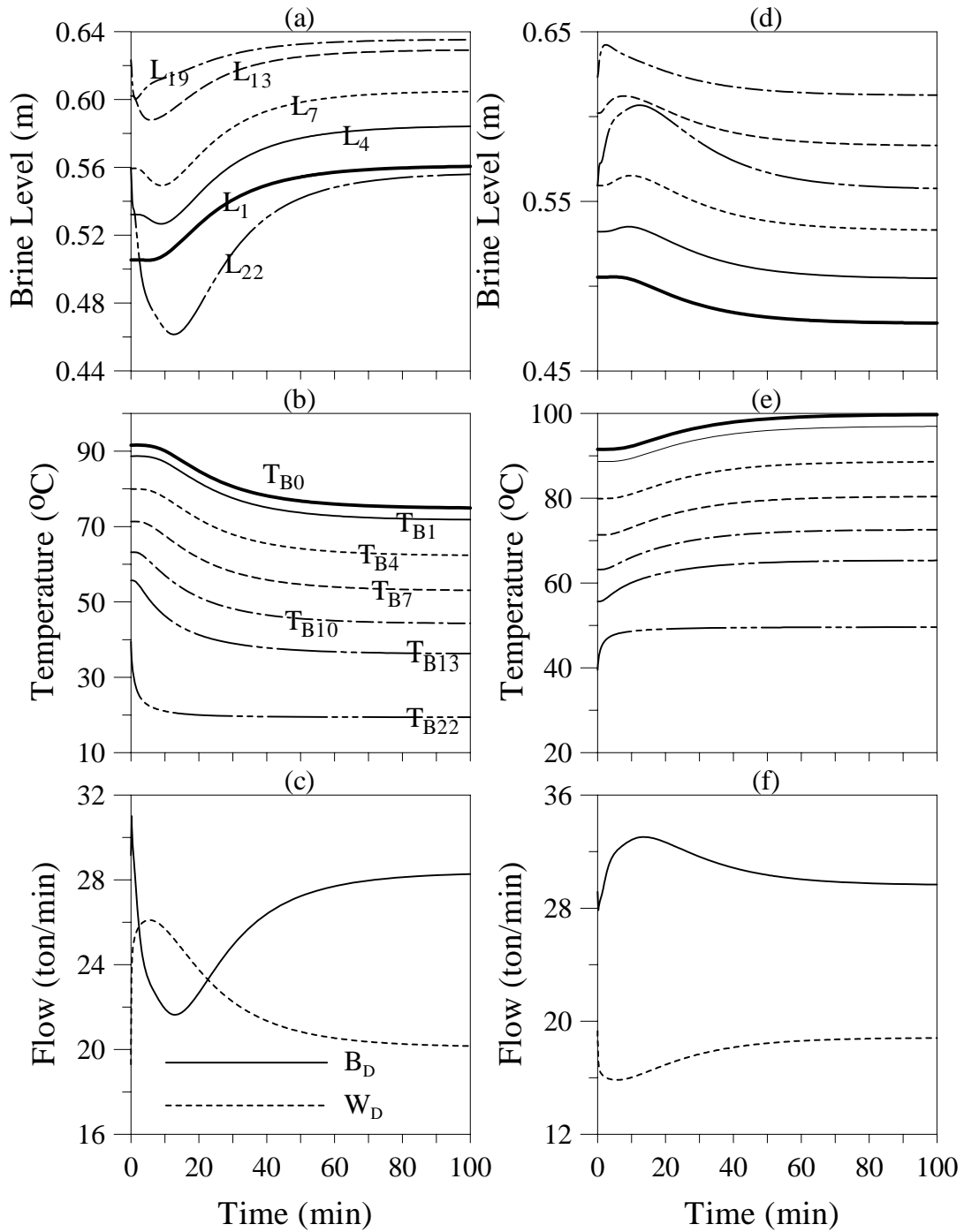


Figure 22: Dynamic response to step change in T_F in open-loop mode, (a-c) $\Delta T_F = -20^\circ\text{C}$; (d-f) $\Delta T_F = +10^\circ\text{C}$.

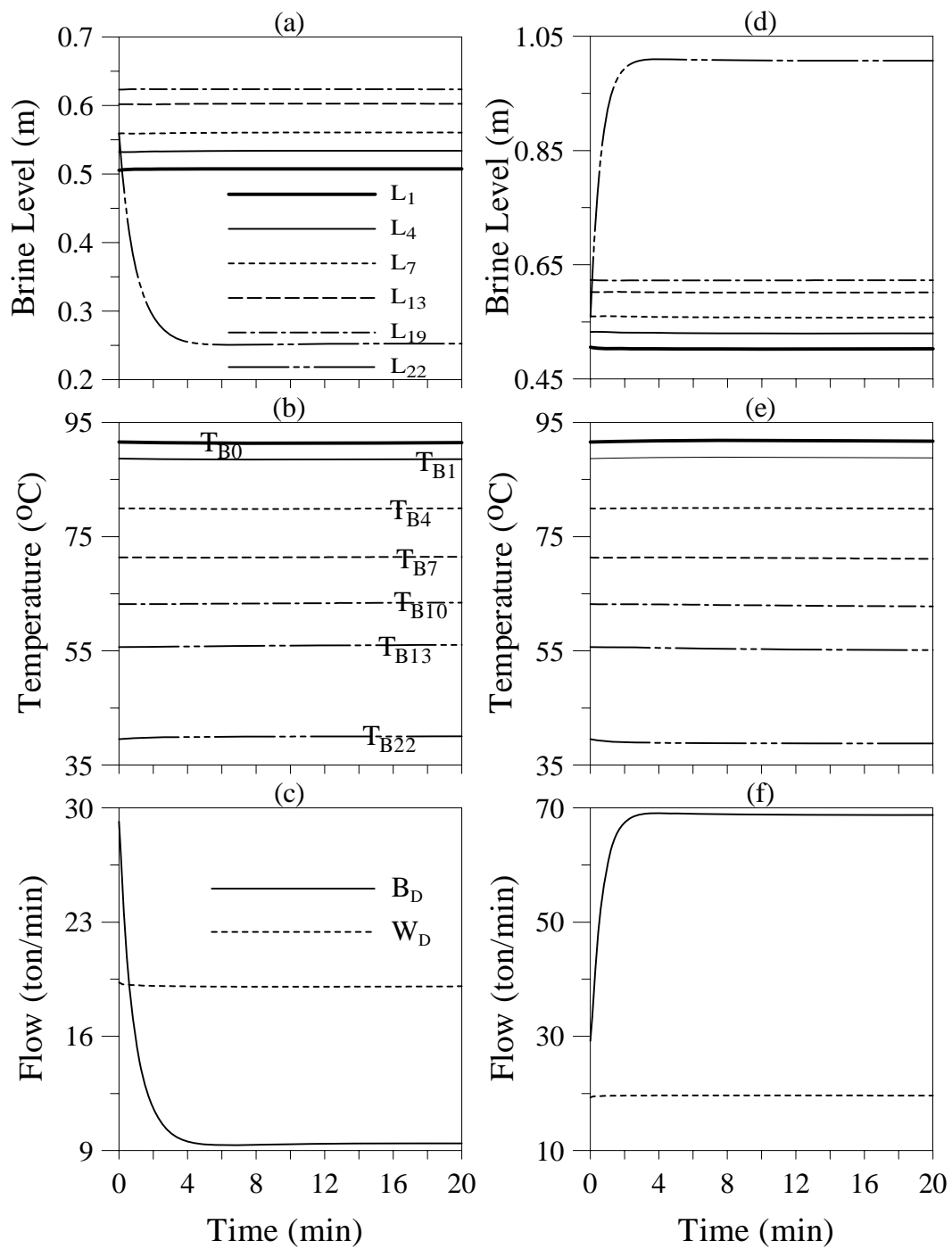


Figure 23: Dynamic response for step change in W_F in open-loop mode, (a-c) $\Delta W_F = -40$ ton/min; (d-f) $\Delta W_F = +40$ ton/min.

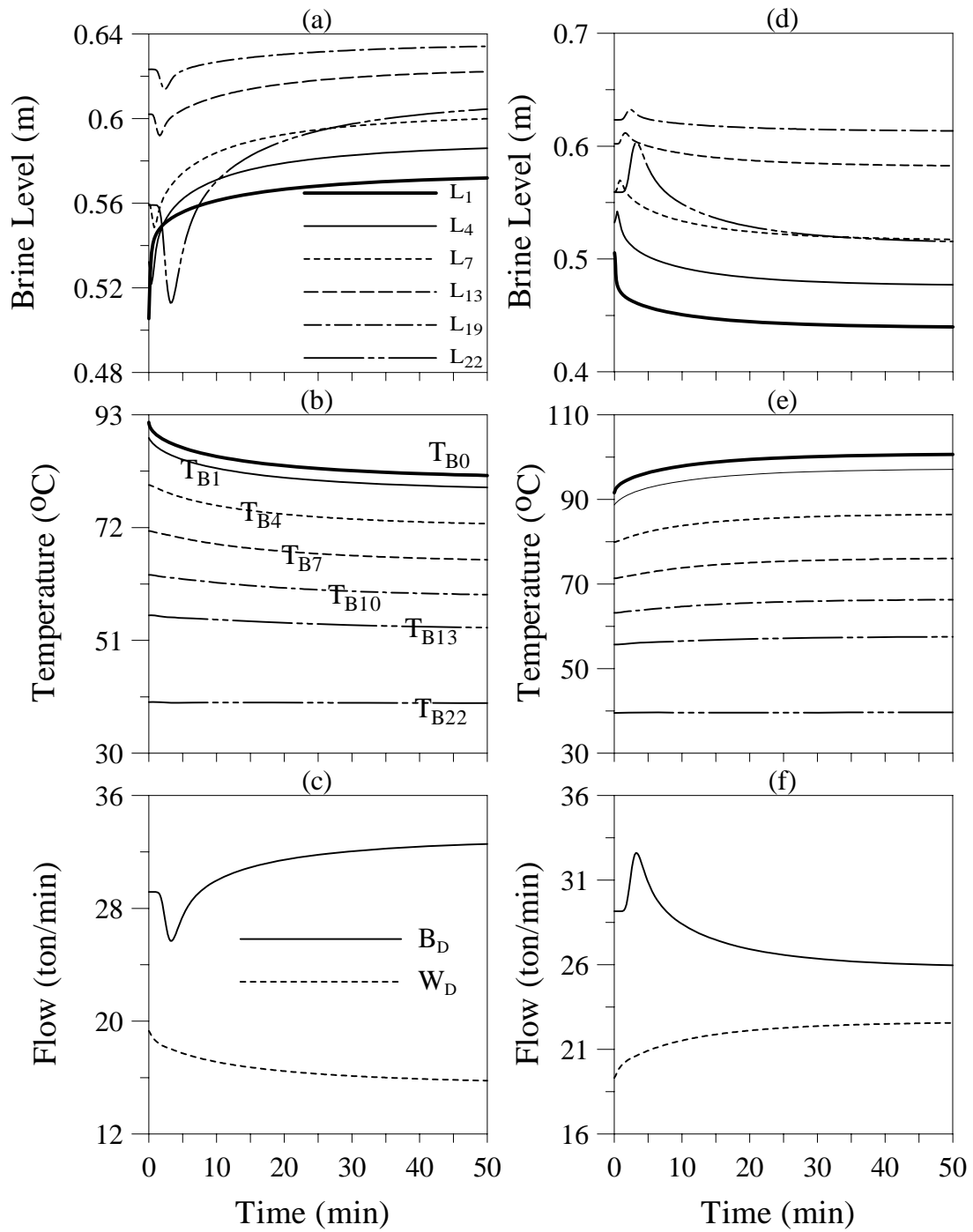


Figure 24: Dynamic response for step change in W_s in open-loop mode, (a-c) $\Delta W_s = -500$ kg/min; (d-f) $\Delta W_s = +500$ kg/min.

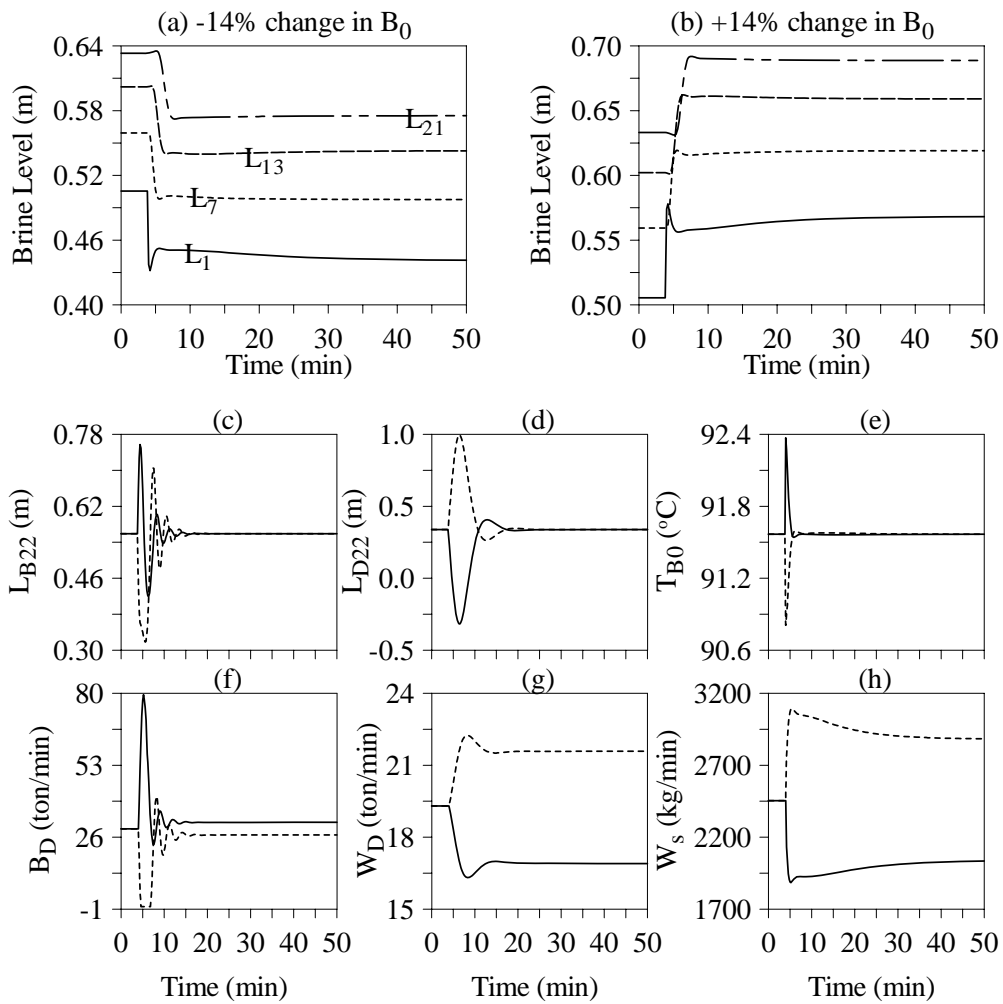


Figure 25: Closed-loop response to $\pm 14\%$ step change in B_0 , (c-h) positive change: dashed line; negative change: solid line.

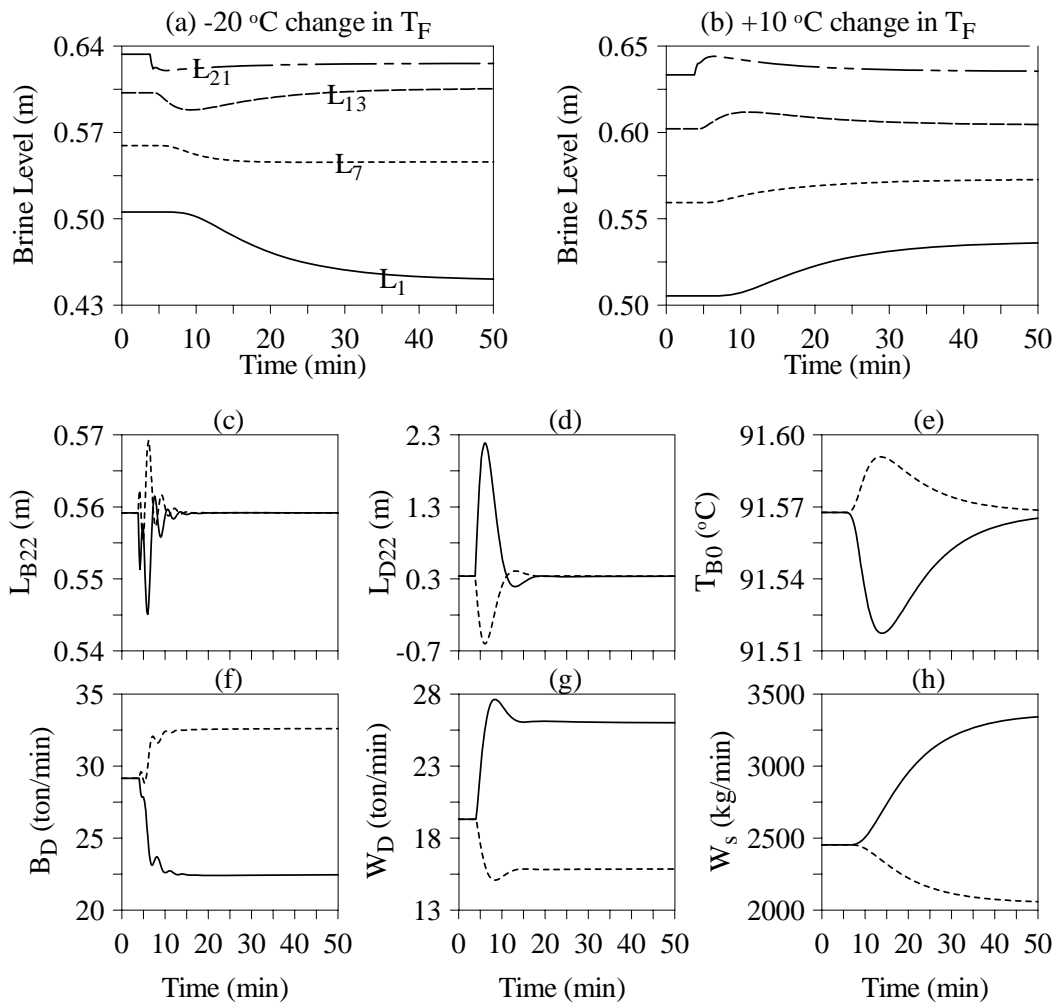


Figure 26: Closed-loop response to -20 and $+10\text{ }^\circ\text{C}$ step change in T_F , (c-h) positive change: dashed line; negative change: solid line.

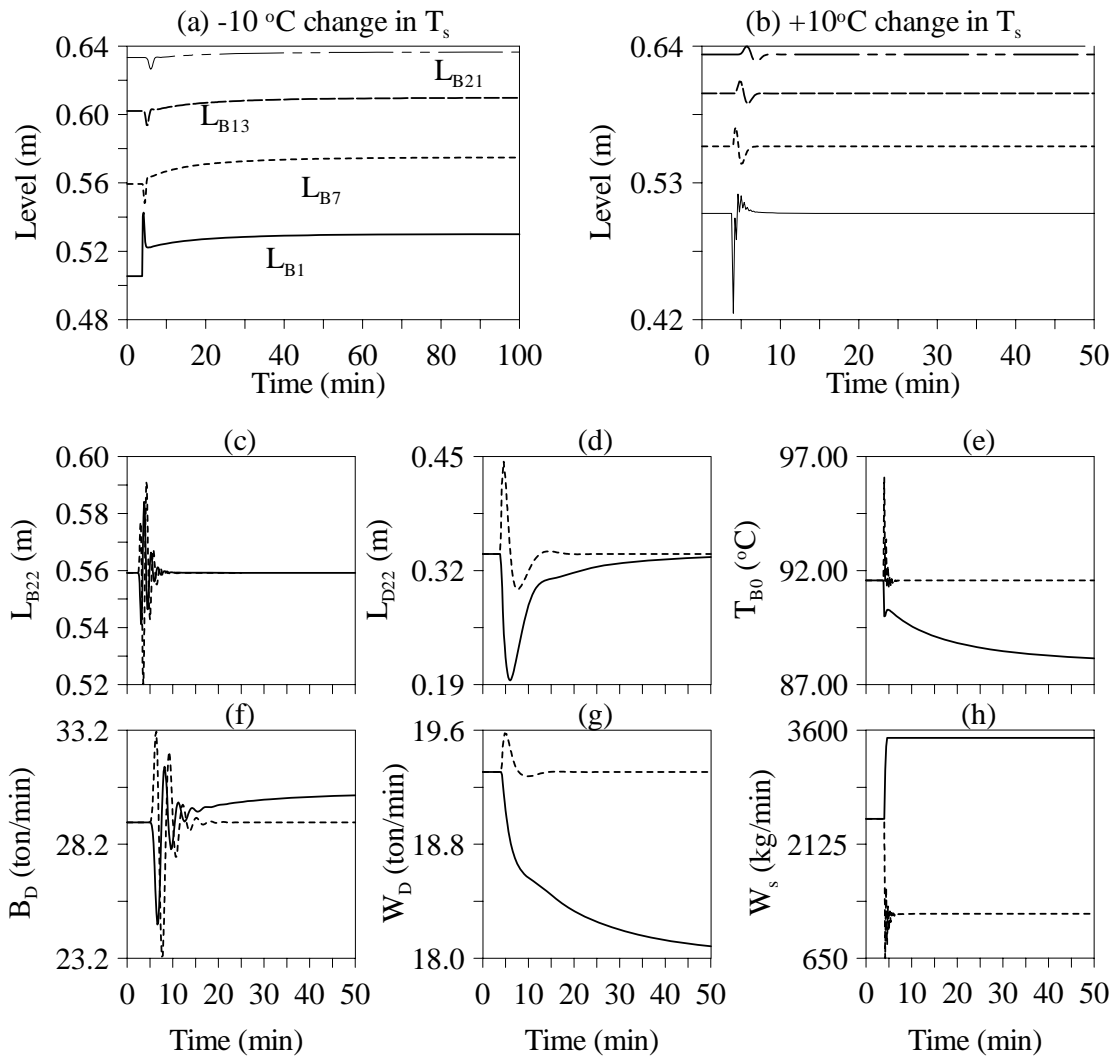


Figure 27: Closed-loop response to ± 10 °C step change in T_s , (c-h) positive change: dashed line; negative change: solid line.

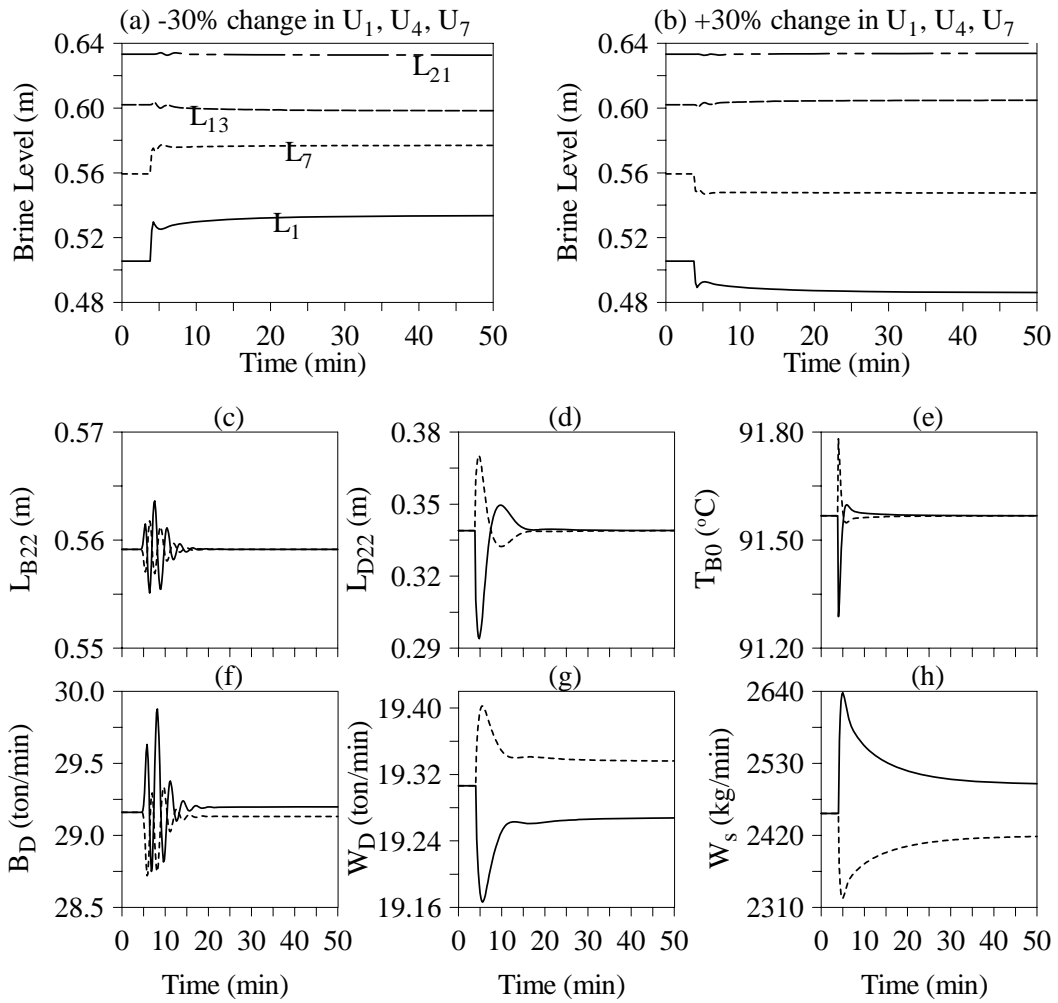


Figure 28: Closed-loop response to $\pm 30\%$ step change in U_1, U_4, U_7 , (c-h) positive change: dashed line; negative change: solid line.